Sedimentary Geology 415 (2021) 105861

Contents lists available at ScienceDirect

Sedimentary Geology

journal homepage: www.elsevier.com/locate/sedgeo

Middle Eocene carbonate platforms of the westernmost Tethys

Manuel Martín-Martín [a,*], Francesco Guerrera [b], Josep Tosquella [c], Mario Tramontana [d]

[a] Departamento de Ciencias de la Tierra y Medio Ambiente, University of Alicante, Alicante, Spain
[b] Ex-Dipartimento di Scienze della Terra, della Vita e dell'Ambiente (DiSTeVA), Università degli Studi di Urbino Carlo Bo, Urbino, Italy
[c] Departamento de Ciencias de la Tierra, University of Huelva, Huelva, Spain
[d] Dipartimento di Scienze Pure e Applicate (DiSPeA), Università degli Studi di Urbino Carlo Bo, Urbino, Italy

ARTICLE INFO

Article history:
Received 24 November 2020
Received in revised form 8 January 2021
Accepted 9 January 2021
Available online 17 January 2021

Editor: Dr. Brian Jones

Keywords:
Lutetian-Bartonian
Carbonate ramps
Sierra Espuña
Internal Betic Zone
Larger benthic foraminifera
Paleoenvironmental evolution

ABSTRACT

A study of the paleoenvironmental evolution of the middle Eocene platforms recognized in the westernmost Tethys has been carried out in the well-exposed middle Eocene succession from Sierra Espuña-Mula basin (Betic Cordillera, S Spain). Eight microfacies (*Mf1* to *Mf8*) have been recognized, based mainly on fossil assemblages (principally larger benthic foraminifera), and rock texture and fabric. The fossiliferous assemblage can be assigned to the 'subtropical' heterozoan association or to the low-latitude 'foralgal facies', which are dominated by non-framework building, light-dependent biota such as perforate larger benthic foraminifera, coralline algae, and sometimes green algae and solitary corals. Larger benthic foraminifer assemblages, corresponding from euphotic to oligophotic conditions and the large surface showed, suggest a progressive marine ramp under essentially oligotrophic conditions. Eventually, supply of detrital sediments from the continent and/or upwelling currents increases the nutrients of marine waters. Comparison with other Tethyan sectors allows stating that coral-reef buildups (z-corals) were widespread on shallow platforms of the central and eastern Tethys Ocean, but these were neither of great dimensions nor dominant because of the much more dominant presence of larger benthic foraminifera. Moreover, these coral constructions were completely absents in the westernmost Tethys. The dominance of larger benthic foraminifera and the absence of z-corals in the westernmost Tethys are explained by particular paleogeographic features due to the occurrence of a narrow and deep oceanic branch (i.e., the Maghrebian Flysch Basin) connecting the Tethys with the Atlantic Ocean. The various issues regarding the morphological characters and evolution of larger benthic foraminifera in the study area, such as sizes of tests, specific diversity and/or intraspecific variability, number of appearances and last occurrences during the middle Eocene are analyzed and compared with those appearing in other Tethyan sectors. In addition, the early to late Bartonian boundary is recognized in the study area as critical for the biological change as in other shallow-marine environments along the Tethys margins.

1. Introduction

The predominance of larger benthic foraminifera (LBF) in the shallow-marine carbonate environments of the Tethys throughout the Eocene was favored by high temperatures (Fig. 1). This caused the reduction of other groups as zooxanthellate corals (z-corals) that instead dominated during the Paleocene (Scheibner and Speijer, 2008; Pomar et al., 2017). Z-corals and LBF, as well as algal symbiont-bearing and specialized organisms (k-strategists), being competitors occupy very similar ecological niches. These groups required favorable ecological conditions such as light, nutrients and euphotic and oligotrophic marine habitats, and also, tropical to subtropical water temperature (Hottinger, 1983; Hallock, 1985, 2000). Nevertheless, LBF are better adapted than corals to unfavorable conditions of higher temperatures, UV exposure and/or presence of nutrients (Hallock, 2000; Scheibner and Speijer, 2008; Payros et al., 2010; Pomar et al., 2017; Sarkar, 2017). This is explained since symbiont algae in corals also tend to be expelled out of the coral tissue, causing bleaching in the corals when a temperature threshold is exceeded (Glynn, 1996; Hallock, 2000; Höntzsch et al., 2013; Pomar et al., 2017). A reduction of LBF has been indicated in literature (Prazeres et al., 2017), when very low light levels conditions and in inorganic nutrient-very rich waters occur together.

During the middle Eocene, from 49 to 45 Ma to the earliest middle Eocene, (Shallow Benthic Zone 14: SBZ 14) warm periods occurred with minor hyperthermal events (middle Eocene Climatic Optimum: MECO; late Lutetian Thermal Maximum: LLTM; Bohaty and Zachos, 2003; Edgar et al., 2007; Sexton et al., 2011; Westerhold et al., 2018; Rivero-Cuesta et al., 2019, 2020) (Fig. 1). This period followed the sharp rise of temperatures at the onset of the Eocene (Kennett and Stott, 1991; Zachos et al., 2008) and the early Eocene Climatic Optimum (EECO; Zachos et al., 2008) (Fig. 1). These warm conditions were maintained until the climate cooling, which occurred at the Eocene-Oligocene boundary (Zachos et al., 1996).

* Corresponding author.
E-mail address: manuel.martin@ua.es (M. Martín-Martín).

https://doi.org/10.1016/j.sedgeo.2021.105861
0037-0738/

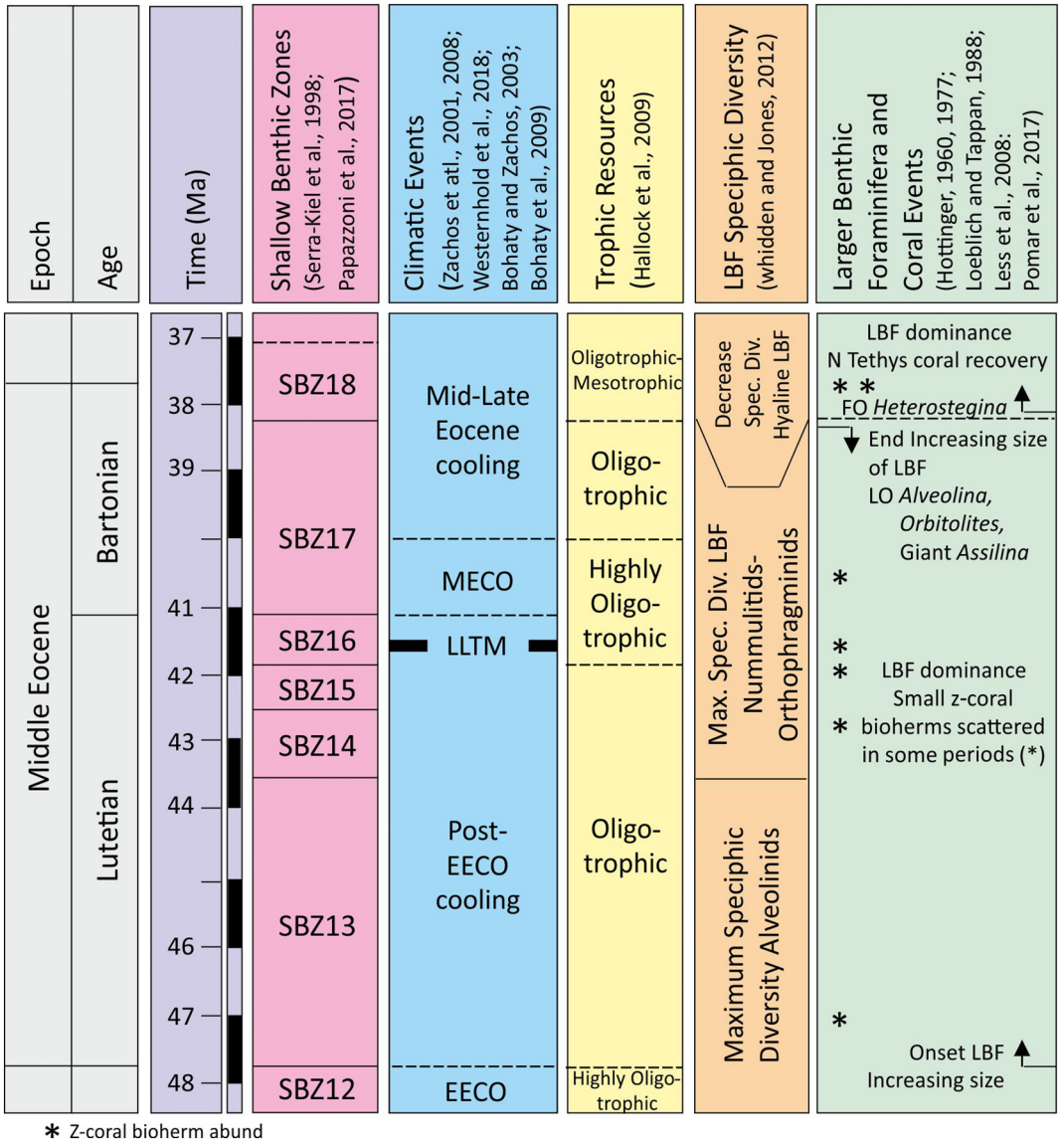

Fig. 1. Chart with the middle Eocene epochs, ages, numerical time scale, shallow benthic zones (SBZ), main climatic events, trophic resources, LBF specific diversity and LBF and coral events.

Wide shallow-marine carbonate platforms developed during the Eocene in the circum-Tethyan sectors. In these broad carbonate shallow-marine areas, larger benthic foraminifera (LBF) rim facies developed (Fig. 1), which were dominated by nummulites and coralline algae. Contrarily, coral patch-reef usually decreased or disappeared during these warming events. In fact, some authors consider that the peaks of great diversification of LBF were mainly related to warm periods, thus giving less importance to the nutrient availability (Scheibner et al., 2005; Whidden and Jones, 2012) or to sea-level rises that increased the area of the biotope and the emergence of new ecological niches (Ungaro, 1994). In this way, a hyperthermal event in the early Lutetian (Fig. 1) coincides in the Tethyan area with the development of alveoline-rich shallow inner ramps thus justifying the peak in specific diversity of alveolinids (Hottinger and Drobne, 1988; Serra-Kiel et al., 1998a; Whidden and Jones, 2012; Pomar et al., 2017). The middle Lutetian to Bartonian time span was a period characterized by an extensive development of hyaline LBF-rich facies, forming large and thick nummulite banks. They developed on the temperate northern Tethyan margin of the N Spain (Pyrenees), at paleolatitudes around 38°N, in Italy, at paleolatitudes around 35°N (Philip et al., 2013), and in localities of the southern Tethyan margin, on the Africa-Arabian shelf, at paleolatitudes between 10°N and 20°N (Höntzsch et al., 2013). Coeval, small to medium-scale coral patch-reefs have been described in the Pyrenean region above the nummulite banks (Martín-Martín et al., 2001) preceding the main phase of coral-reef buildups developed at the middle-late Eocene transition (late Bartonian-early Priabonian). This feature is recorded in numerous localities of the circum-Tethyan region with the progressive cooling in the post-MECO interval (Perrin and Kiessling, 2010; Höntzsch et al., 2013; Pomar et al., 2017).

Eocene carbonate platforms developed in the Betic-Rif orogen both in the internal Malaguide-Ghomaride domain, at paleolatitudes around 25°N (Serrano et al., 1995; Martín-Martín, 1996; Martín-Martín et al., 1997a, 1997b; Martín-Martín et al., 2020c) and in the Prebetic units of the External Betic Zone (Geel et al., 1998; Geel, 2000; Höntzsch et al., 2013; Guerrera et al., 2014), at paleolatitudes around 30°N. The fossil Malaguide-Ghomaride shallow-marine areas represented the transition to the proto-Atlantic domain at low latitudes, in a paleogeographic area still little studied.

The post-Cretaceous paleogeography of the westernmost Tethyan domain shows that the western Mediterranean area was characterized by different oceanic branches the most important of which was represented by the Maghrebian Flysch Basin (MFB). This basin was connected with a sector of the proto-Atlantic Ocean at the present corresponding to a portion of the Betic-Rifian Gibraltar Arc (Guerrera and Martín-Martín, 2014; Guerrera et al., 2021; Martín-Martín et al., 2020a, 2020b).

Changes in the fossiliferous assemblages and the evolution of the LBF deduced from the stratigraphic sections studied allow establishing both environmental changes and the biogeographic content (Hottinger, 1983; Brasier and Bosence, 1995). The use of biozones based on characteristic LBF assemblages allows extracting sedimentary, paleoenvironmental, paleoclimatic and paleoceanographic information.

The Sierra Espuña area displays one of the most complete and well-exposed Paleogene shallow-marine successions of the Betic-Rif Chain and neighboring Mediterranean areas (Fig. 2A, B). This research

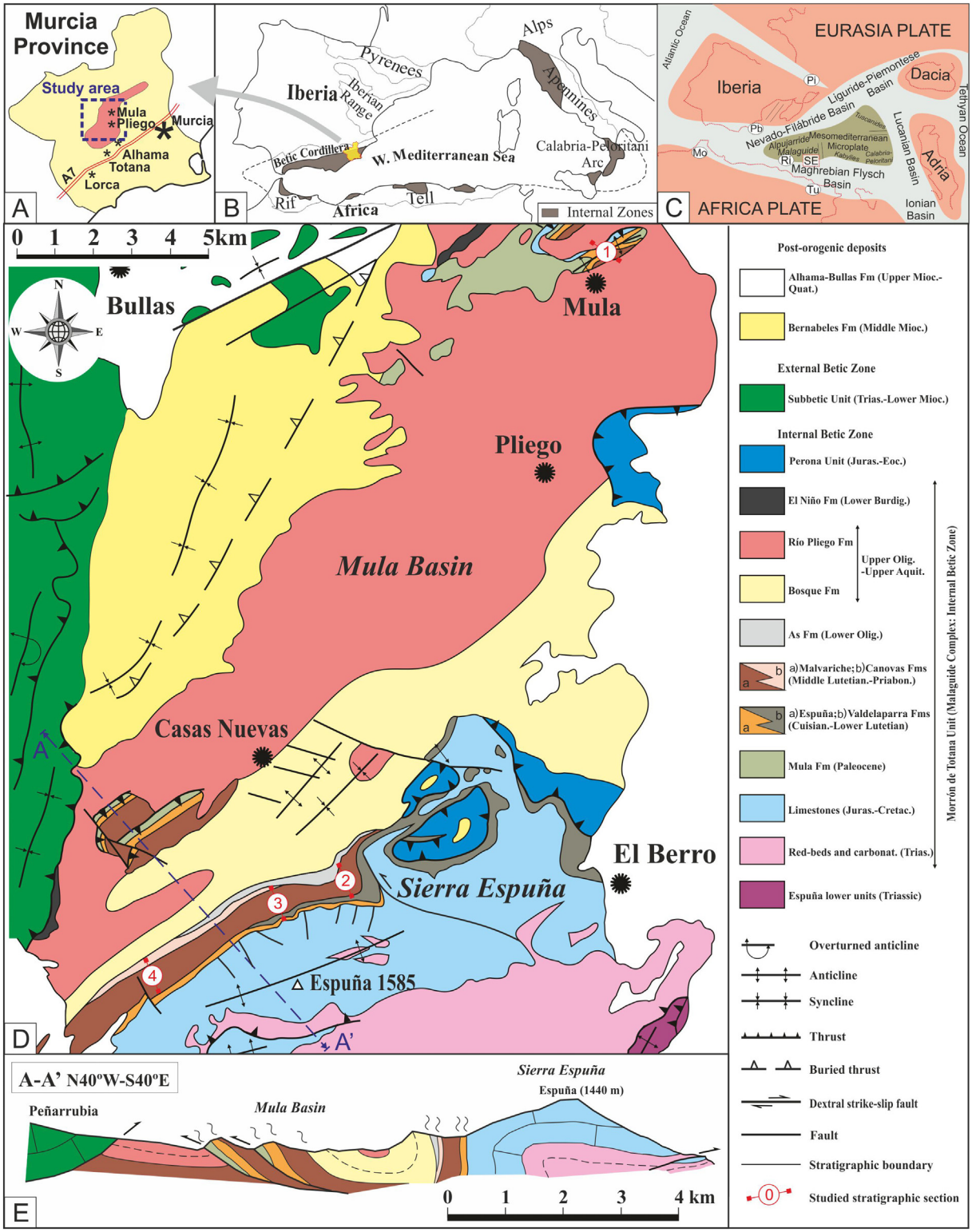

Fig. 2. A) Location of the study area in the Murcia Province (SE Spain). B) Western Mediterranean Alpine chains with location of the Murcia Province in the Betic Cordillera. C) Paleogeographic sketch of the western Mediterranean area at the late Cretaceous (after Guerrera and Martín-Martín, 2014) with the location of the study area (SE), Pyrenean domain (Pi), Prebetic domain (Pb), Rifian domain (Ri), Moroccan domain (Mo) and Tunisian domain (Tu). D) Geological map of the Sierra Espuña-Mula basin area with the location of the geological cross section shown in E and the studied stratigraphic sections (1 to 4); E) Geological cross section.

presents the description and interpretation of micro- and macro-facies of four stratigraphic sections from the middle Eocene outcropping in this area. The biostratigraphic analyses are based on benthic communities living in shallow-marine waters and, in particular, on larger benthic foraminifera. On the basis of the biozonation by Serra-Kiel et al. (1998a), a precise dating of the LBF associations recognized in the study area was published by Serra-Kiel et al. (1998b). This permits reconstructing the main evolutionary stages of the LBF, which then helps in the paleoenvironmental interpretation of the middle Eocene carbonate shallow-marine areas. Our results reveal significant differences and coincidences of these Middle Eocene carbonate platforms of the Betic Cordillera, located at paleolatitudes around 25°N and around 10°W, when compared with results concerning other Tethyan sectors.

2. Background

2.1. Geology

The Betic Cordillera is part of the westernmost Alpine Chain in the Mediterranean area (Fig. 2B). The birth of this mountain chain system is derived from the closing of several Tethyan oceanic branches and the collision of different microplates against the Iberia-Eurasia and Africa plates (Fig. 2C) (Wildi, 1983; Martín-Algarra, 1987; Doglioni, 1992; Guerrera et al., 2005; Guerrera and Martín-Martín, 2014; Guerrera et al., 2021; Martín-Martín et al., 2020a, 2020b).

The area considered corresponds to the Sierra Espuña-Mula basin which exposes a well-developed Meso-Cenozoic sedimentary succession belonging to the Morrón de Totana Tectonic Unit of the Malaguide Complex (Internal Betic Zone), one of the upper tectonic units involved in the structure of the Sierra Espuña area. This sedimentary succession comprises several stratigraphic formations grouped in two cycles (pre-orogenic: Paleocene-Early Oligocene; syn-orogenic: Late Oligocene-Burdigalian) (Figs. 2D, 3). The middle Eocene stratigraphic record of the Morrón de Totana Unit (Fig. 2D, 3) comprises four formations: the Espuña, Valdelaparra, Malvariche, and Canovas fms. The Malvariche Fm unconformably rests above the Espuña and Valdelaparra Fms (Cuisian-Lower Lutetian in age). In turn, the Malvariche Fm shows a lateral and upward transition to the Canovas Fm (Martín-Martín, 1996; Martín-Martín et al., 1997a, 1997b, 1998; Serra-Kiel et al., 1998b; Martín-Martín et al., 2006; Martín-Martín and Robles-Marín, 2020).

The tectonic structure of the Morrón de Totana Unit (Fig. 2E) is constituted by an antiformal stack followed northward by a syncline including several thrust sheets in the Mula Basin, which in turn northward contacts with the External Betic Zone by a backthrusting over the Internal Zone.

2.2. Stratigraphy

Stratigraphic-biostratigraphic studies carried out in the Espuña, Valdelaparra, Malvariche, and Cánovas Fms provided a detailed stratigraphic architecture (Fig. 3) including LBF, planktonic foraminifera and calcareous nannoplankton dating from literature. These data allow an accurate chronologic control of the middle Eocene sedimentation in the area. In the present work, the biostratigraphic data (Fig. 4) by Serra-Kiel et al. (1998b) based on the Shallow Benthic Zones (SBZ, Serra-Kiel et al., 1998a) and modifications by Papazzoni et al. (2017) for the LBF are followed. The planktonic foraminifera and calcareous nannoplankton data by Martín-Martín (1996) and Martín-Martín et al. (1997a, 1997b) were integrated in a chronologic framework according to the Geologic Time Scale (Gradstein and Ogg, 2012). In the considered area, the boundaries between the middle Eocene formations are marked by lithological changes and an unconformity surface at the base of the middle Lutetian (Fig. 3). The middle Eocene sedimentation is represented by two couples of heteropic formations, which are separated by an unconformity surface at the early-middle Lutetian boundary (Martín-Martín et al., 1997a, 1997b).

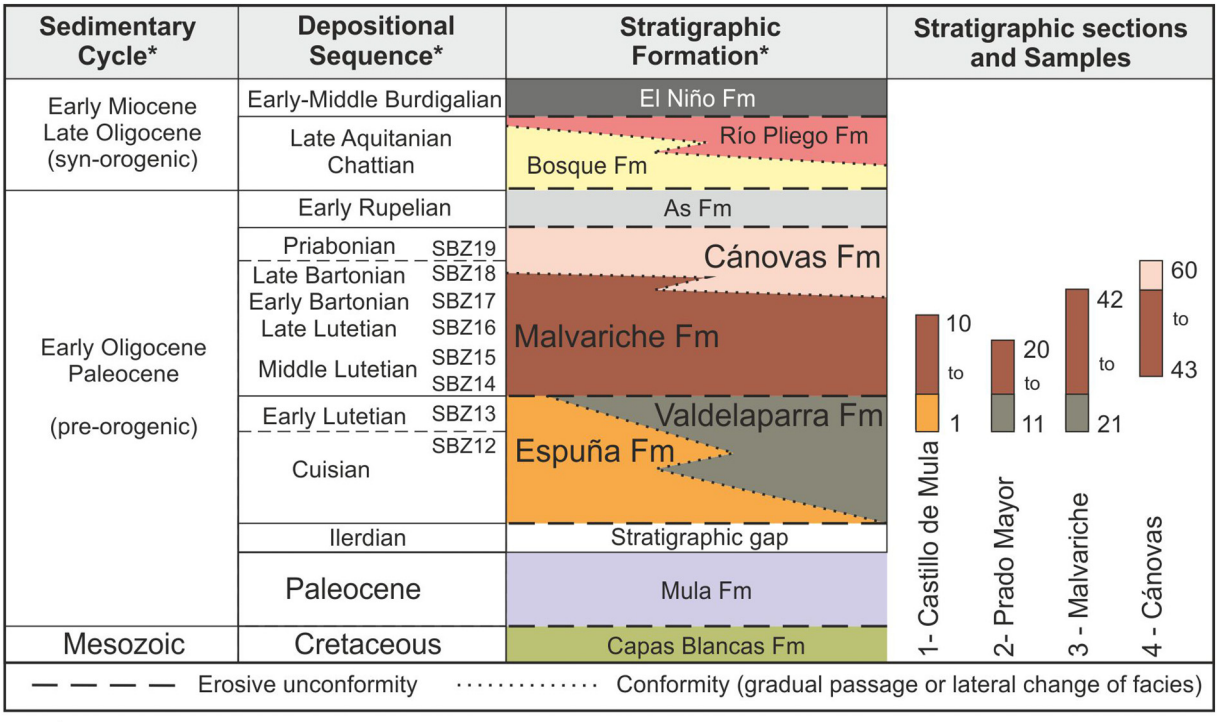

Fig. 3. Stratigraphic framework of the Tertiary succession of the Sierra Espuña-Mula Basin area.

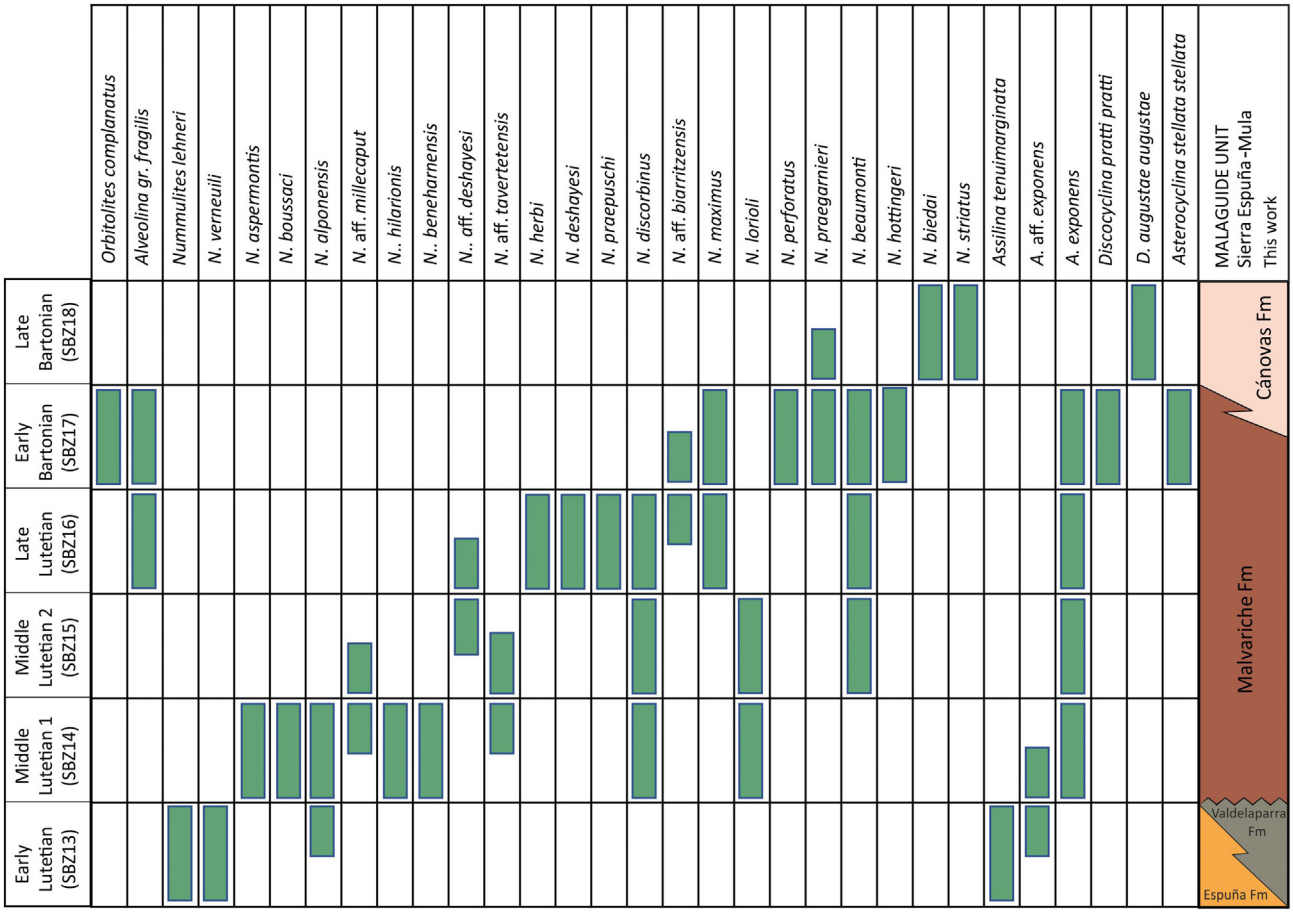

Fig. 4. Biochronostratigraphic distribution and stratigraphic range of larger benthic foraminifera recognized in the middle Eocene deposits of the study area based on data from Serra-Kiel et al. (1998a), revised and updated.

The lower couple of stratigraphic formations is Ypresian to early Lutetian in age (Martín-Martín et al., 2020c), but in this work, only the early Lutetian portion has been studied. These formations are: (a) the Espuña Fm, which crops out in the entire study area and is represented by inner to outer ramp deposits consisting of limestones and/or calcarenites with numerous LBF, and open marine marly sandstones, siltstones and marls with deeper benthic foraminifers, planktonic foraminifers and calcareous nannoplankton; (b) the Valdelaparra Fm, which crops out in the Prado Mayor and Malvariche sections and represents a lagoonal to marshy inner ramp environment. The upper two heterotopic formations (middle Lutetian to Priabonian in age) resting above an unconformity (Martín-Martín et al., 1997a, 1997b) are: (c) the Malvariche Fm (middle Lutetian to late Bartonian), which crops out in the entire study area and is constituted by an inner to outer ramp facies consisting of limestones and/or calcarenites with numerous LBF, and open marine marly sandstones, siltstones and marls with deeper environment benthic foraminifers, planktonic foraminifers and calcareous nannoplankton; (d) the Cánovas Fm (late Bartonian to Priabonian), which represents a more distal unit. This formation is composed of middle to outer ramp deposits, consisting in the lowermost part of limestones and/or calcarenitic beds with common LBF, that evolve in the middle and upper part of the formation to sandy marls, silts and marls alternating with calcarenite beds with abundant planktonic foraminifers and calcareous nannoplankton.

The LBF association analyzed in the Malvariche Fm covers a time span extending from the middle Lutetian to the early Bartonian (SBZ 14–17). Planktonic foraminifers and calcareous nannoplankton observed in the middle part of this unit belong to the P12-P14 and NP18–20 zones, respectively (Martín-Martín, 1996; Martín-Martín et al., 1997a, 1997b). On the other hand, the LBF assemblage from the Cánovas Fm spans from the early Bartonian to the early Priabonian (SBZ 17–19). The presence in the nannoplankton association of *Chiasmolithus oamaruensis* suggests a late Eocene age for the upper levels of the Cánovas Fm, not documented by LBF.

The sedimentary cycles, depositional sequences (stratigraphic bodies separated by unconformity surfaces), and formations of the Mula-Sierra Espuña basin and their lateral relationships are summarized in Fig. 3.

2.3. Paleoplatforms in the Betic Cordillera

In the Betic Cordillera, the middle Eocene neritic deposits are only represented in the External (Prebetic) and the Internal (Malaguide) zones (southeastern Spain). In the External Subbetic zone, the middle Eocene consists mainly of pelagic and turbidite deposits (Grupo Cardela and Capas Rojas Fm.; Vera, 2000). In this period, the area between the Iberian and African plates and the Mesomediterranean microplate, the so-called 'flysch trough' (Vera, 2000) or Maghrebian Flysch Basin (Guerrera et al., 2014), is characterized only by turbidite sedimentation.

Shallow-marine Prebetic successions of middle Eocene age are mainly described in the Onil, Ibi, Carrasqueta and Penaguila sections of the Alicante region (Geel et al., 1998; Geel, 2000; Höntzsch et al., 2013) and in the Internal Prebetics from the Jaen-Albacete provinces (Jerez, 1981). In the same domain of the Murcia and Albacete sectors, shallow carbonate deposits are represented by Nummulite-, Alveolina- and algae-rich marine limestones (Jerez, 1981; Vera, 2000). Finally, sediments of an imprecise middle Eocene age and related to an analogous depositional setting are also recognized in the Jumilla-Cieza area (Murcia region). In this area, a shallowing-upwards sequence developed in

Table 1
Lithostratigraphic data of the studied stratigraphic sections with the representation of the interval thickness, name of formation, samples collected, age, fossils visible to the naked eye and lithofacies description (Martín-Martín, 1996; Martín-Martín et al., 1997a, 1997b; Serra-Kiel et al., 1998a).

Stratigraphic section 1 (Log 1) – locality: Castillo de Mula (Mula Basin)

Thickness (m)	Formation	Samples	Age	Field lithofacies	Fossils recognized in the field	Microfacies
5	MALVARICHE (75 m)	9–10	Late Lutetian *p. p.* (SBZ16)	***Lithofacies M9*:** prevalent limestones and/or calcarenites and yellowish-reddish sandy marls with occasional Fe—Mn nodules	Algae	**Mf1**
40		6–7–8	Middle Lutetian (SBZ15)	***Lithofacies M8*:** conglomeratic beds yellowish sandy marls alternation and reduction of calcareous blocks and nodules		**Mf2**
30		3–4-5	Middle Lutetian (SBZ14)	***Lithofacies M7*:** prevalent chaotic conglomerates and calcareous blocks		**Mf1**
Erosion surface						
0,1–03	ESPUÑA (>20 m)		Early Lutetian (SBZ13)	***Lithofacies M6*:** as below, but here between two decametric ocraceous nodular discontinuous levels		**Mf1**
10		1–2				
0,2–0,4						
>10			Cuisian (SBZ12)	***Lithofacies M6*:** discontinuous biocalcarenites (fine to coarse grained matrix)	Frequent flat Nummulites (gr. Millecaput); size of Nummulites and Assilines can reach and exceed 3–5 cm; algae	

Stratigraphic section 2 (Log 2) – locality: Prado Mayor (Sierra Espuña Basin)

Thickness (m)	Formation	Samples	Age	Field lithofacies	Fossils recognized in the field	Microfacies
130	MALVARICHE (75 m)	19–20	Middle Lutetian (SBZ15) *p.p.*	***Lithofacies I1 + I2. I1:** as below*; ***I2:*** similar to **I1** but here with Nummulites	**I2:** not flat but globulose Nummulites.	**Mf2**
		16–17				
		−18				
100		15	Middle Lutetian *p.p.* (SBZ15-SBZ14)	***Lithofacies H3:** as below*	Gastropod-rich micritic limestones (freshwater or transitional environment)	**Mf3**
130		13–14	Middle Lutetian *p.p.* (SBZ14)	***Lithofacies I1:*** alternating frequent decametric and pluri-decimetric biocalcarenite beds and pelitic-sandy beds		**Mf2**
Erosion surface						
30	VALDELA-PARRA (>180)	12	Early Lutetian (SBZ 13)	***Lithofacies H3:*** yellowish gray homogeneous silty-sandy pelites; occasional muscovite-rich quartzose arenites with carbonate cement. Pelites/(arenites + limestones) ratio is about 95/5; instead the pelites/limestones ratio is about 70/30	Gastropod-rich micritic limestones (freshwater or transitional environment**)**	**Mf3**
120		–		*Semicovered interval*		
>30		11	Cuisian (SBZ12)	***Lithofacies G:*** amalgamated grayish-blackish and brownish micritic limestones with indistinct bedding	Abundant Miliolids, occasional Alveolines and Orbitolides; the association indicates a very restricted environment (e.g. estuary, lagoon, marsh)	

Stratigraphic section 3 (Log 3) – locality: Malvariche (Sierra Espuña Basin)

Thickness (m)	Formation	Samples	Age	Field lithofacies	Fossils recognized in the field	Microfacies
16	MALVARICHE (490 m)	40–41–42	Early Bartonian (SBZ17)	***Lithofacies S:*** bioclastic limestones	Small Nummulites and probable Ostreids and Echinoderms	**Mf2**
4		39		***Lithofacies N:*** as below		**Mf4**
5		38		***Lithofacies R:*** as below		**Mf5**
5		37	Late Lutetian (SBZ 16)	***Lithofacies N:*** as below		**Mf4**
10		36		***Lithofacies R:*** very cemented biocalcarenites (fine to medium grained and with much larger fossils); presence of brecciated structures	*Nummulite perforates*, N. *planes*, encrusting organisms, elongated Alveolines; fossiliferous intraclasts	**Mf5**
		35				**Mf7**
		34				**Mf2**
6		–		*Semicovered interval*		
74		33		***Lithofacies O:*** as below		
50		–		*Semicovered interval*		**Mf4**
25		32		***Lithofacies N:*** as below		
15		30–31	Middle Lutetian (SBZ 15)	***Lithofacies O + Q:*** as below		**Mf2**
15				***Lithofacies Q:*** lens shaped, poorly stratified brecciated biocalcarenites	Very frequent Ostreids (size 5–10 cm), Nummulites, Discocyclines, Assilines, Annelids, Lamellibranches	
10		29		***Lithofacies N + P. N:** as below; **P:***		**Mf4**
10		27–28		***Lithofacies O:*** lenticular bodies of medium-grained biocalcarenites with a brecciated structure	Frequent fossils of (various cm in size) including Discocyclines, grouped in lenses of different dimensions	**Mf2**
5		26		***Lithofacies N:*** as below		**Mf4**
75		24–25	Middle Lutetian (SBZ 14)	***Lithofacies M:*** alternating limestones and sandy-pelites with Nummulites; brecciated limestone beds in the upper portion	Large Nummulite and *Alveoline aff. fusiformis* (2–3 cm at least); Algae and Rodolites	**Mf6** **Mf5**

Table 1 (*continued*)

Stratigraphic section 3 (Log 3) – locality: Malvariche (Sierra Espuña Basin)

Thickness (m)	Formation	Samples	Age	Field lithofacies	Fossils recognized in the field	Microfacies
38				***Lithofacies N:*** yellowish homogeneous silty-sandy pelites	Abundant Assiline and Nummulites	**Mf4**
2		–		*Semicovered interval*		
		25		22–23	***Lithofacies I:*** metric thick beds of stratified biocalcarenites (medium to coarse grained)	Abundant
	Nummulites (diameter 1.5–2 cm), Assiline, Echinoderms,			Lamellibranches	**Mf2**	
Erosion surface						
35	VALDELA-	–	Early	***Lithofacies H1-H3.*** **H1:** described below; **H3:** described in log 2.		
5	PARRA	21	Lutetian	***Lithofacies H:*** micritic massive limestones	Gastropods	
60	(>220)	–	(SBZ 13)	***Lithofacies H1:*** yellowish-gray homogeneous silty-sandy pelites and occasional decimetric muscovite-rich quartzose arenites, with a carbonate cement, (pelites/arenites ratio = 95/5); occasional micritic limestones		**Mf3**
80		–		*Semicovered interval*		
>40		–	Cuisian (SBZ12)	***Lithofacies G:*** similar characteristics checked in the Log 2		

Stratigraphic section 4 (Log 4) – locality: Cánovas (Sierra Espuña Basin)

Thickness (m)	Formation	Samples	Age	Field lithofacies	Fossils recognized in the field	Microfacies
30	CÁNOVAS (100 m)	59–60	Priabonian (SBZ19)	***Lithofacies Y:*** unstratified brownish to pinkish silty-marls with planktonic foraminifers and characterized by the absence of larger foraminifera.	Planktonic foraminifers, absence of larger foraminifera	**Mf4**
30		57–58	Late Bartonian (SBZ18)	***Lithofacies W:*** brownish silty-marls, occasional metric calcarenite beds	Discocycline (of a deeper environment than the Assiline); Discocycline and occasional Operculine	**Mf8**
20		–		*Semicovered interval*		
20		55–56		***Lithofacies Z:*** fossiliferous sands	Abundant Assiline	
40	MAIVARICHE (340 m)	52–53-54	Early Bartonian (SBZ17)	***Lithofacies U:*** as below		**Mf2**
25		51	Late Lutetian (SBZ16)	***Lithofacies T:*** as below		**Mf4**
7		50		***Lithofacies U:*** as below		**Mf8**
18		49		***Lithofacies T + N.*** ***T:*** as below; **N:** as Log 3		**Mf4**
65		47–48		***Lithofacies Q:*** as Log 3		
50		45–46	Middle Lutetian (SBZ15)	***Lithofacies U:*** poorly stratified bioclastic limestones and limestones (fine grained; 50 m thick); the size of fossils is much larger than the grain size of the limestones; sometimes abundant carbonaceous frustules.	Corals, deep Ostreids, Gastropods (e.g. Turritellids); the size of fossils is much larger than the grain size of the limestones; carbonaceous frustules.	**Mf8**
15		–		***Lithofacies Q:*** as Log 3		
40		–		***Lithofacies T***: as below		
20		44		***Lithofacies Q:*** as Log 3		
50		43		***Lithofacies T:*** unstratified brownish silty-marls	Planktonic foraminifers, corals and solitary corals, large and flat Nummulites, Lamellibranches, Gastropods (e.g. Turritella), sometimes fossils are isooriented producing a pseudo-lamination	

this period testifies an evolution from inner marine platform to continental settings (Sierras del Carche, Enmedio, Benis and Caramucel; Kenter et al., 1990).

In the Alicante region, in the northeastern part of the Betic Cordillera, the Paleogene sedimentation is extremely variable due to the complex paleogeography of the area, which is controlled by the onset of tectonic uplift of the Betic orogen. Shallow-marine deposits are mainly distributed in the northern sector of the region, passing southward to external platform and slope deposits. The morphology of the platform is highly compartmentalized, generating deposits and interspersed erosion surfaces in different sedimentary settings. Geel et al. (1998) recognized a wide early-middle Eocene platform in the westernmost Onil-Ibi-Carrasqueta areas that would constitute an uplifted block with a shallow-marine sedimentation. For the late middle Eocene, these authors recognized an additional carbonate platform in the northernmost Alcoy, Penaguila and Sierra de Aitana areas. A tectonic tilting of the region at the end of this period caused an emersion and erosion of the highest parts of the succession, marking the end of the middle Eocene sedimentation (Kenter et al., 1990; Geel et al., 1998). Regarding the sequence-stratigraphy interpretation, Geel (2000) described in detail the middle Eocene deposits of the Ibi-Onil and Penaguila areas, recognizing in the Ibi section, the most developed and representative shallow-marine platform for this time, and five shallowing-upwards depositional cycles of mainly hyaline LBF-rich limestones (nummulites, assilines and discocyclines) limited by sequence boundaries mainly controlled by tectonics and sea-level changes. The middle Eocene shallow-marine deposits are also widely represented in the Internal (Malaguide) zone of the Sierra Espuña (Murcia) area, and they have been studied in the present work. Around the city of Malaga, possible coeval deposits are recognizable in the 'Chaotic Complex', which includes larger alveolinid limestone blocks in olistostrome-like structures of marine slope environments (Serrano et al., 1995).

3. Methods and materials

The methodology applied in the study area consists of classic field observations and sampling, laboratory analyses, and interpretation. The field observations were aimed at characterizing the sedimentary lithofacies of the studied stratigraphic successions. The laboratory study was aimed to the characterization of the various middle Eocene biofacies and to a relative estimation of fossil components and, in particular, of the biochronostratigraphic distribution of the larger benthic foraminifera (LFB). The collected data allow a paleoenvironmental interpretation and a reconstruction of their evolution. In addition, a new geological map (Fig. 2D) shows the different formations, the tectonic elements, and the location of the studied stratigraphic sections (Castillo de Mula, Prado Mayor, Malvariche and Cánovas). A geological cross section showing the thrust-and-fold structure of the area is reported in Fig. 2E. The involved stratigraphic formations (Espuña, Valdelaparra, Malvariche and Cánovas Fms) belonging to the Malaguide Complex (Internal Betic Zone) have been measured for a total thickness of 1695 m.

Different litho-biofacies have been recognized (Table 1). A total of 60 samples have been analyzed in order to the microfacies characterization (Figs. 5, 6 and 7), both as hand samples and as thin-sections (3 to 8 thin-sections for each sample). Paleoecological and depositional paleoenvironment characteristics have been defined by the study of standard thin-sections by means of a Nikon optical microscope model Eclipse E 200. In order to characterize the microfacies, photographs were taken with a Nikon digital camera model DS-Fi2, transferred with a camera controller to a PC and treated using a Nikon software (Digital Sight DS-U3, NIS Elements F4).

The microfacies analysis (Figs. 6 and 7) has been carried out using the method of Flügel (2010): (1) description of lithology; (2) grain type (skeletal/non skeletal); (3) grain size and sorting; (4) textures; and (5) microfossil assemblages. For the microfacies, denomination and carbonate classification were followed (Dunham 1962).

Loeblich and Tappan (1987) have been followed for the taxonomic classification of nummulitids (genus *Assilina* includes *Assilina* s.s. and operculiniform *Assilina* from Tosquella and Serra-Kiel, 1998). The marine paleoenvironment reconstruction is carried out using the ramp subdivision terminology according to Burchette and Wright (1992) and Pomar (2001), but also considering the photic subdivisions according to Pomar et al. (2017), so that the 'mesophotic zone' appears. In particular, the uppermost boundary of this mesophotic zone could coincide with the lower limit of the 'uppermost photic zone' of Hottinger (1997) and the deepest occurrence of marine vegetation (Pomar, 2001). In turn, the lowermost boundary could coincide with the lower limit of the 'upper photic zone' of Hottinger (1997) at near 80 m of depth, with the onset of a large benthic foraminifera assemblage dominated by orthophragminids (Hottinger, 1997). Finally, the Nebelsick and Bassi (2000) terminology has been used when samples contained crustose coralline red algae.

4. Results

4.1. Litho- and biostratigraphy

The main lithofacies features of the middle Eocene successions have been reconstructed by means four stratigraphic sections (logs) measured in the Mula-Sierra Espuña Basins (Figs. 2D, 3) and their descriptions are summarized in Fig. 5 and Table 1. Log 1 has been measured in the Mula Basin (Castillo de Mula locality) and the other three logs in the Sierra Espuña area (in the localities Prado Mayor, log 2; Malvariche, log 3; and Cánovas, log 4). In the four stratigraphic sections, sixty samples have been collected, which are distributed as follows: ten (1 to 10) in the Castillo de Mula section; ten (11 to 20) in the Prado Mayor section; twenty-two (21 to 42) in the Malvariche section; and eighteen (43 to 60) in the Cánovas section.

4.1.1. Stratigraphic section 1 (Castillo de Mula)

The succession of this log, belonging to the Mula Basin, extends over 85 m from the upper part of the Espuña Formation to the Malvariche Formation, from the Cuisian (SBZ12) to the late Lutetian (SBZ 16, *p.p.*).

In this stratigraphic section, the lower ten meters, which belong to the Espuña Fm (*Lithofacies M6*, early Lutetian/SBZ13), are topped by an unconformity marked by a 10–30 cm thick yellowish Fe-hydroxydes mineralized bed probably related to an emersion. The *Lithofacies M6* consists of discontinuous fine- to coarse-grained biocalcarenites, with frequent flat nummulites (e.g. N. gr. *millecaput-maximus*) and red algae. The dimensions of nummulites and assilines can reach and exceed 3–5 cm. This level was dated (Martín-Martín et al., 1997a, 1997b) as early Lutetian (SBZ13) with the LBF assemblage consisting of *Nummulites lehneri*, *N. verneuili*, *N. alponensis*, *Assilina tenuimarginata* and *A. aff. exponens* (Fig. 4).

Above the unconformity surface, the stratigraphic section shows 75 m of the Malvariche Fm constituted by three main stratigraphic intervals (*Lithofacies M7*, *M8* and *M9*), characterized by various lithofacies (Fig. 5, Table 1).

The Malvariche Fm is interrupted at the top by a tectonic contact (fault at the core of a syncline in whose limb the log has been measured). This formation is made up of chaotic conglomerate blocks that pass to less chaotic and stratified matrix-supported conglomerates, with a calcareous mud matrix (re-mobilized in situ) alternating with yellowish sandy marls and algal biocalcarenites. The limestone clasts gradually decrease upwards until they disappear in the last 10–15 m of the succession.

Three main stratigraphic intervals have been recognized in this formation: (i) *Lithofacies M7* (lower portion, 30 m thick; middle Lutetian *p.p.*/SBZ14), where chaotic conglomerates and calcareous blocks prevail; (ii) *Lithofacies M8* (middle portion, 40 m thick; middle Lutetian *p.p.*/SBZ15), characterized by alternating conglomeratic beds and yellowish sandy marls and by a reduction of calcareous blocks; (iii) *Lithofacies M9* (upper portion, 5 m thick; late Lutetian *p.p.*/SBZ16), prevalently represented by amalgamated algal biocalcarenites and yellowish-reddish sandy marls with occasional Fe—Mn nodules.

The early middle Lutetian (SBZ14) was dated (Martín-Martín et al., 1997a, 1997b) with the LBF assemblage consisting of *Nummulites aspermontis*, *N. boussaci*, *N. alponensis*, *N. aff. millecaput*, *N. hilarionis*, *N. beneharnensis*, *N. aff. tavertetensis*, *N. discorbinus*, *N.lorioli*, *A. aff. exponens* and *A exponens* (Fig. 4). This level was followed by the late middle Lutetian (SBZ15) dated by Martín-Martín et al. (1997a, 1997b) with the LBF assemblage consisting of *N. aff. millecaput*, *N. aff. deshayesi*, *N. aff. tavertetensis*, *N. discorbinus*, *N.lorioli*, *N. beaumonti* and *A exponens* (Fig. 4). The LBF assemblage consisting of *Alveolina gr. fragilis*, *N. aff. deshayesi*, *N. herbi*, *N. deshayesi*, *N. praepuschi*, *N. discorbinus*, *N. aff. biarritzensis*, *N. maximus*, *N. beaumonti* and *A exponens* (Fig. 4) allowed to date the late middle Lutetian (SBZ16) (Martín-Martín et al., 1997a, 1997b) to the top of this stratigraphic section. In the stratigraphic section 1, two main microfacies (*Mf1*, *Mf2*), described afterwards, have been recognized.

4.1.2. Stratigraphic section 2 (Prado Mayor)

This stratigraphic section (Sierra Espuña Basin, Log 2, more than 520 m thick) is made up by the upper portion of the Valdelaparra Fm (more than 160 m) and the Malvariche Fm (360 m thick) extending from the Cuisian (SBZ12) to middle Lutetian (SBZ15) where different lithofacies have been recognized (Fig. 5 and Table 1). The early middle Lutetian (SBZ14) was dated (Martín-Martín et al., 1997a, 1997b) with the LBF assemblage consisting of *Nummulites aspermontis*, *N. boussaci*, *N. alponensis*, *N. aff. millecaput*, *N. hilarionis*, *N. beneharnensis*, *N. aff. tavertetensis*, *N. discorbinus*, *N.lorioli*, *A. aff. exponens* and *A exponens* (Fig. 4). The LBF assemblage consisting of *N. aff. millecaput*, *N. aff.*

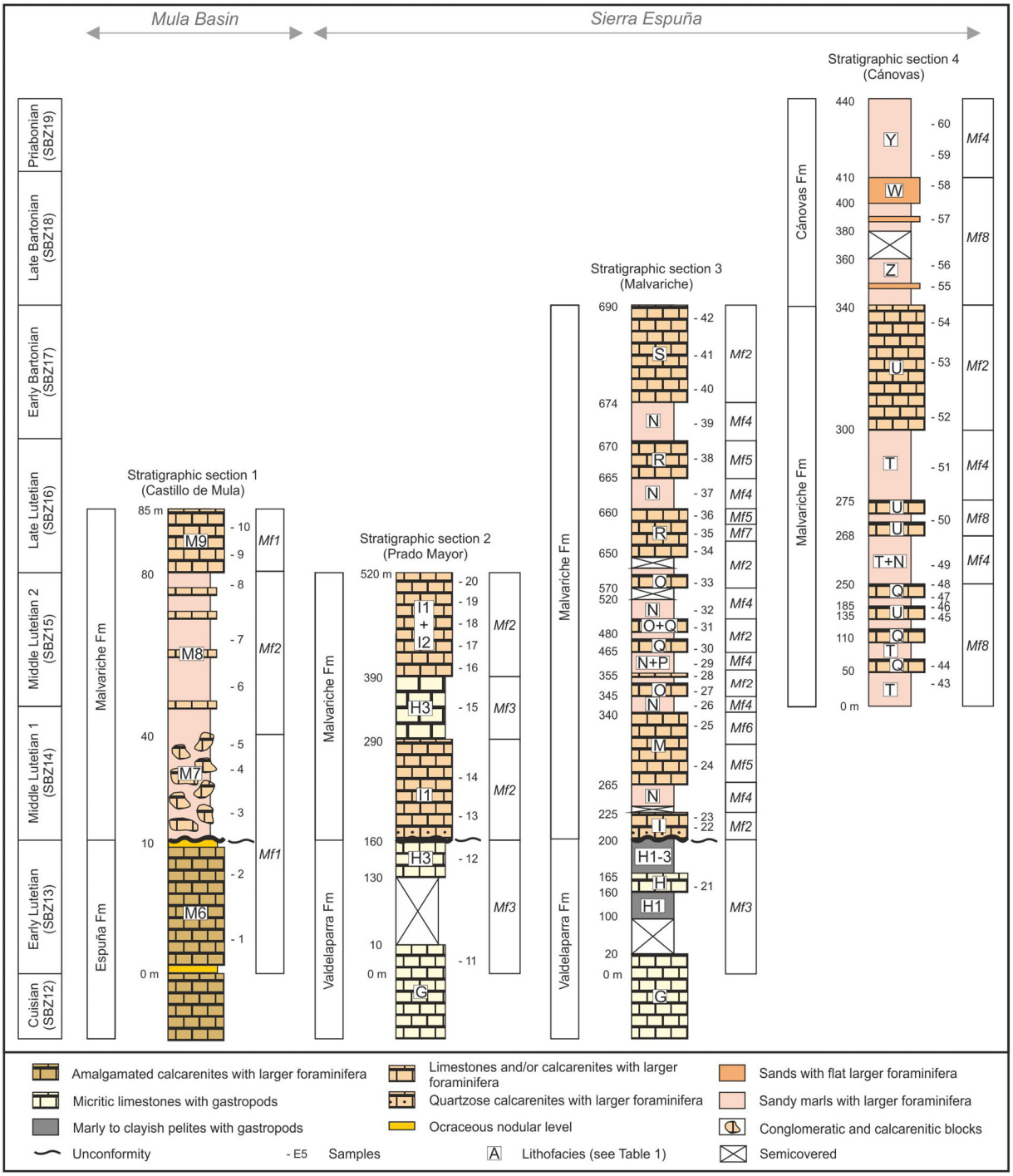

Fig. 5. Studied stratigraphic sections represented as columns. Sections have different scales because Section 1 is much thinner than the others. The distribution of defined lithofacies and microfacies (*Mf1* to *Mf8*), and the location of studied samples are represented.

deshayesi, *N. aff. tavertetensis*, *N. discorbinus*, *N.lorioli*, *N. beaumonti* and *A exponens* (Fig. 4) allowed to date the late middle Lutetian (SBZ15) (Martín-Martín et al., 1997a, 1997b).

The lower *Lithofacies G* (Cuisian/SBZ12-early Lutetian/SBZ13 *p. p.*) of the Valdeparra Formation, analyzed in detail for ten meters, shows grayish-blackish and brownish amalgamated micritic limestones with indistinct bedding, containing abundant miliolids and occasional alveolines and orbitolites, whose fossil association indicates a very restricted environment (e.g. estuary, lagoon, marsh). The following early Lutetian *p.p. Lithofacies H3* (Valdelaparra Fm) observed for 30 m (after a semicoverd interval of 120 m) shows homogeneous yellowish-gray silty-sandy pelites with occasional decimetric muscovite-rich quartzose arenites, carbonate cement and occasional micritic limestones with abundant freshwater or brackish gastropods. In this lithofacies, the pelite/(arenite + limestone) ratio is about 95/5, while the pelite/limestone ratio is about 70/30.

The top of the Valdeparra Fm is represented by an unconformity surface, which separates this formation from the overlying Malvariche Fm, in which three main stratigraphic intervals have been recognized (*Lithofacies I1*, *H3* and *I1 + I2*). *Lithofacies I1* (50 m thick; middle Lutetian/SBZ14 *p.p.*) is represented by frequent decimetric

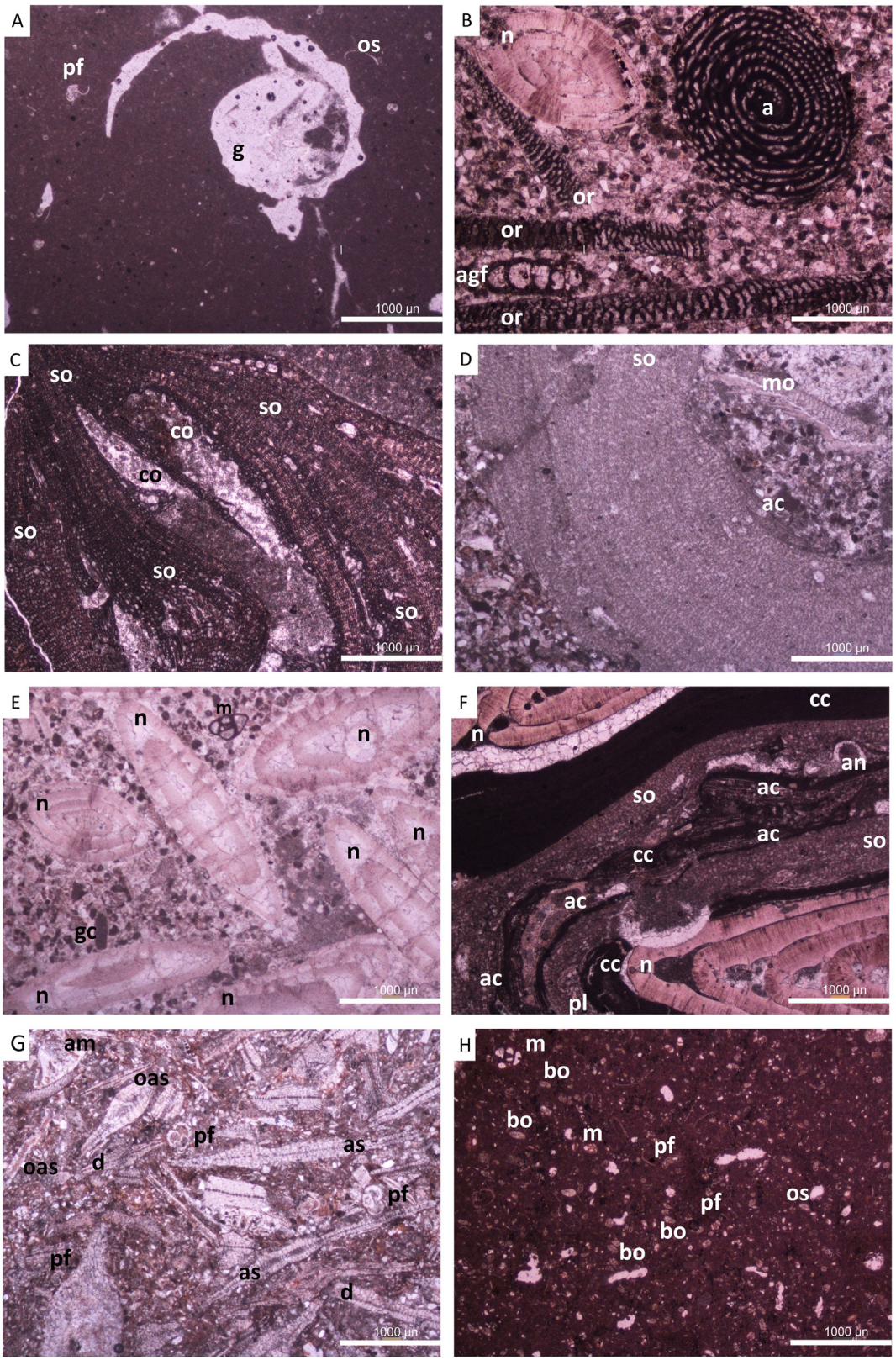

Fig. 6. Photomicrographs of the middle Eocene microfacies of the study area: A) *Mf3* M1: sample 12; B) *Mf5* M2: sample 36; C) *Mf6* M3: sample 25; D) *Mf7* M4: sample 35; E) *Mf2* M5: sample 13; F) *Mf1* M6: sample 3; G) *Mf8* M7: sample 58; H) *Mf4* M8: sample 23. Scale bar: 1000 mm. Key: a, alveolinid; ac, acervulinid; agf, agglutinate foraminifer; am, amphisteginid; an, annelid; as, asterocyclinid; bo, bolivinid; co, colonial coral; cc, crustose coralline algae; d, discocyclinid; g, gastropod; gc, geniculate coralline algae; m, miliolid; mo, mollusk; n, *Nummulites*; oas, operculiniform *Assilima;* or, *Orbitolites*; os, ostracod; pf, planktic foraminifer; pl, planorbulinid; so, solenomeris.

and pluridecimetric biocalcarenite beds alternating with pelitic-sandy beds, which include frequent flattened nummulites. The following 100 m of succession are similar to the previously described *Lithofacies H3* (here middle Lutetian/SBZ14–15 *p.p.*), recognized at the top of the Valdelaparra Fm. The stratigraphic section 2 ends with 130 m of succession consisting of an alternance of *Lithofacies I1* (just described, but here

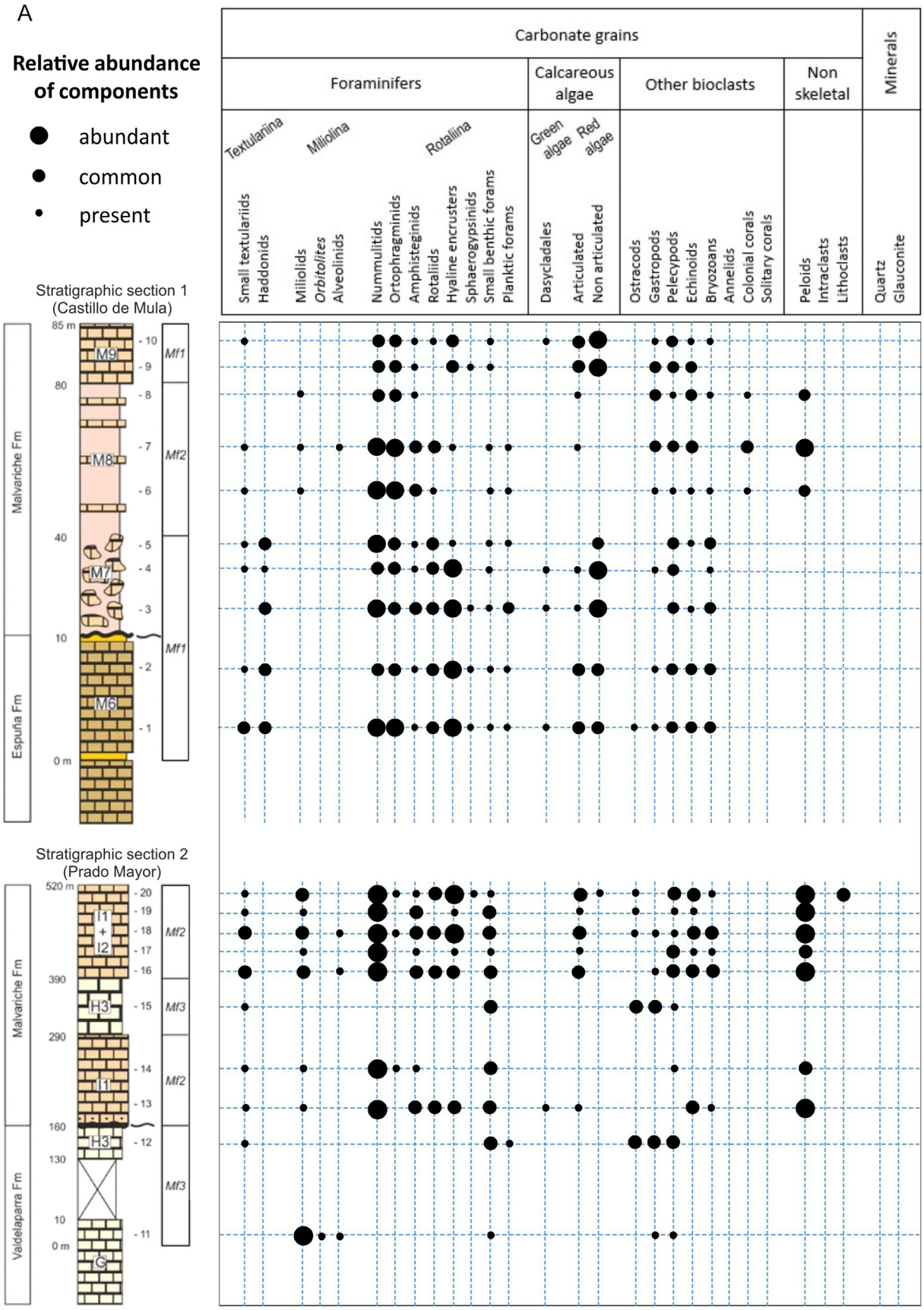

Fig. 7. Relative abundance of components recognized in the studied thin sections a) Stratigraphic Sections 1 (Castillo de Mula) and 2 (Prado Mayor); b) Stratigraphic Sections 3 (Malvariche) and 4 (Cánovas). Component is divided into three categories, according to the relative abundance estimated under the optical microscope: (1) *present* is used when the element is seen at least once in the whole thin-section; (2) *common* is indicated when the element appears at least once using an objective ×4; (3) *abundant* is considered when the element appears 2 to 4 times using an objective ×4.

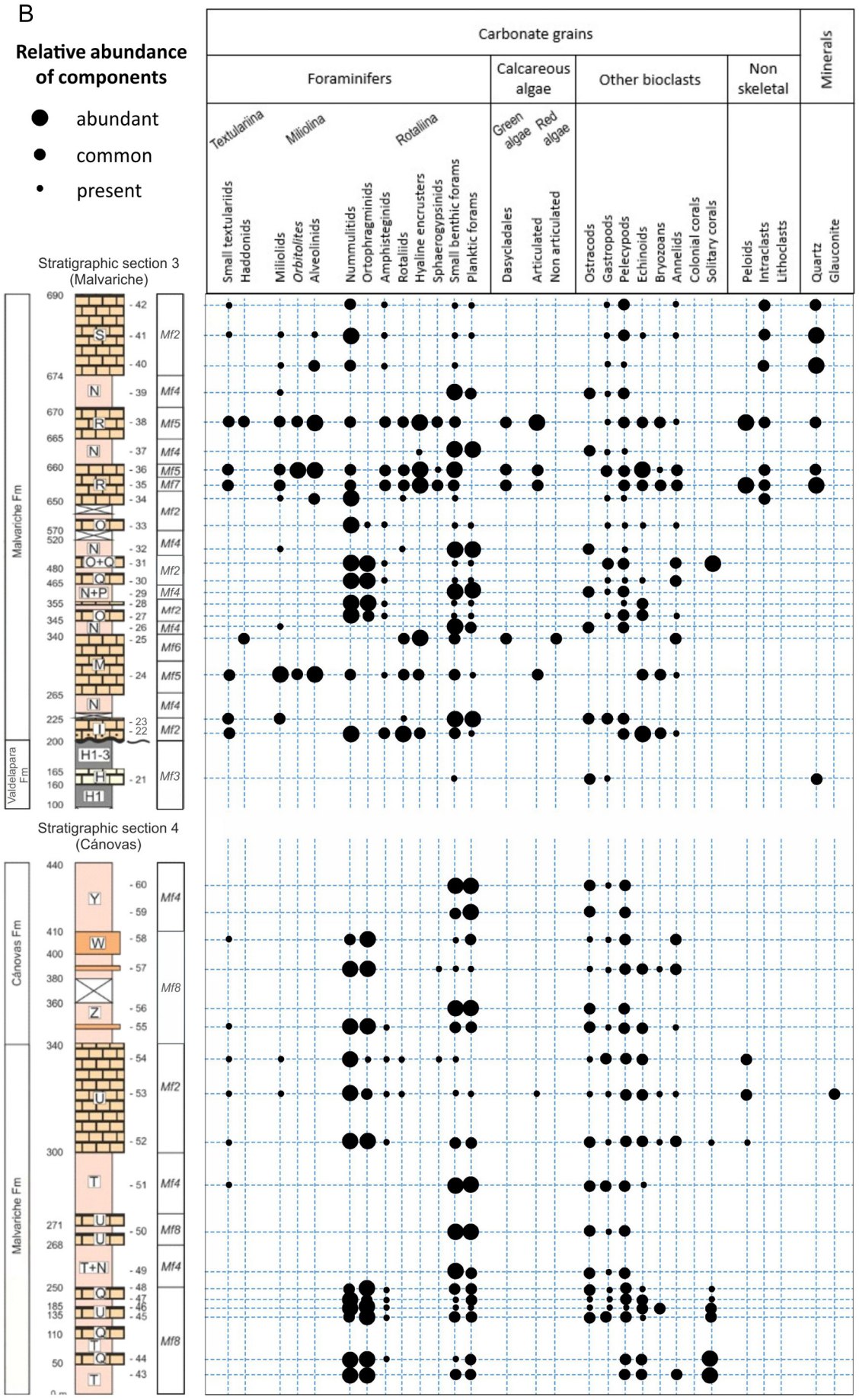
B
Relative abundance of components
abundant
common
present
Carbonate grains
Foraminifers
Calcareous algae
Other bioclasts
Non skeletal
Minerals
Textulariina
Miliolina
Rotaliina
Green algae
Red algae
Small textulariids
Haddonids
Miliolids
Orbitolites
Alveolinids
Nummulitids
Ortophragminids
Amphisteginids
Rotaliids
Hyaline encrusters
Sphaerogypsinids
Small benthic forams
Planktic forams
Dasycladales
Articulated
Non articulated
Ostracods
Gastropods
Pelecypods
Echinoids
Bryozoans
Annelids
Colonial corals
Solitary corals
Peloids
Intraclasts
Lithoclasts
Quartz
Glauconite
Stratigraphic section 3 (Malvariche)
Malvariche Fm
Valdelapara Fm
Stratigraphic section 4 (Cánovas)
Cánovas Fm
Malvariche Fm

middle Lutetian/SBZ15) and *Lithofacies I2*. The latter is similar to I1 but contains globulose nummulites instead the flattened ones.

In the stratigraphic section 2, two main microfacies (*Mf2*, *Mf3*) were recognized, which repeated at different levels of the succession. The characteristics of these microfacies are described afterwards.

4.1.3. Stratigraphic section 3 (Malvariche)

This stratigraphic section (Sierra Espuña Basin, Log 3, more than 690 m thick) comprises the upper portion of the Valdelaparra Fm (more than 200 m thick) and the Malvariche Fm (490 m thick), in an area where different lithofacies have been recognized (Fig. 5 and Table 1). The age of the succession of Log 3 extends from the Cuisian (SBZ12) to the early Bartonian (SBZ17). The early Lutetian (SBZ13) was dated (Martín-Martín et al., 1997a, 1997b) with the LBF assemblage consisting of *Nummulites lehneri*, *N. verneuili*, *N. alponensis*, *Assilina tenuimarginata* and *A. aff. exponens* (Fig. 4). This level is followed by the early middle Lutetian (SBZ14) dated by Martín-Martín et al. (1997a, 1997b) with the LBF assemblage consisting of *Nummulites aspermontis*, *N. boussaci*, *N. alponensis*, *N. aff. millecaput*, *N. hilarionis*, *N. beneharnensis*, *N. aff. tavertetensis*, *N. discorbinus*, *N.lorioli*, *A. aff. exponens* and *A exponens* (Fig. 4). The LBF assemblage consisting of *N. aff. millecaput*, *N. aff. deshayesi*, *N. aff. tavertetensis*, *N. discorbinus*, *N.lorioli*, *N. beaumonti*, and *A exponens* (Fig. 4) allowed to date the following level as late middle Lutetian (SBZ15) (Martín-Martín et al., 1997a, 1997b). The late middle Lutetian (SBZ16) was dated (Martín-Martín et al., 1997a, 1997b) with the LBF assemblage consisting of *Alveolina gr. fragilis*, *N. aff. deshayesi*, *N. herbi*, *N. deshayesi*, *N. praepuschi*, *N. discorbinus*, *N. aff. biarritzensis*, *N. maximus*, *N. beaumonti*, and *A exponens* (Fig. 4). This level is followed by the late middle Lutetian (SBZ16) dated by Martín-Martín et al. (1997a, 1997b) with the LBF assemblage consisting of *Alveolina gr. fragilis*, *N. aff. deshayesi*, *N. herbi*, *N. deshayesi*, *N. praepuschi*, *N. discorbinus*, *N. aff. biarritzensis*, *N. maximus*, *N. beaumonti*, and *A exponens* (Fig. 4). The early Bartonian (SBZ17) was dated (Martín-Martín et al., 1997a, 1997b) with the LBF assemblage consisting of *Orbitolites complanatus*, *Alveolina gr. fragilis*, *N. aff. biarritzensis*, *N. maximus*, *N. perforatus*, *N. praegarnieri*, *N. beaumonti*, *N. hottingeri*, *A exponens*, *Discocyclina pratti pratti* and *Asterocyclina stellata stellata* (Fig. 4). In the lower part of the formation predominates *Lithofacies G* (Cuisian/SBZ12-early Lutetian/SBZ13 *p.p.*). This lithofacies was analyzed over a thickness of twenty meters and shows similar characteristics to those seen in the previous Log 2. After 80 m of semicovered succession ocurrs *Lithofacies H1* (60 m thick). This lithofacies shows homogeneous yellowish-gray silty-sandy pelites with occasional decimetric muscovite-rich quartzose arenites, with a carbonate cement (pelite/arenite ratio = 95/5) and occasional micritic limestones. After five meters of *Lithofacies H*, which consists of micritic massive limestones with gastropods, follow *Lithofacies H1* just described and *Lithofacies H3* described in the previous Log 2, for a total thickness of 35 m.

After the same unconformity surface observed in the previous logs, the succession passes to the Malvariche Fm, within which different lithofacies have been detected. The succession of this formation starts with *Lithofacies I* (25 m thick) characterized by metric beds of medium- to coarse-grained stratified biocalcarenites, rich in nummulites (diameter of 1.5–2 cm) and assilines, and with frequent echinoderms and lamellibranchs. After 2 m of semicovered succession appears *Lithofacies N* (38 m thick) characterized by yellowish homogeneous silty-sandy pelites with a poor macrofossil content. There follows *Lithofacies* M (75 m thick), which consists of limestones with large nummulites and *Alveolina* aff. *fusiformis* (at least 2–3 cm in diameter) alternating with sandy-pelites containing nummulites. The upper portion of this lithofacies shows a biostromal structure constituted by the encrusting foraminifer *Solenomeris*. *Lithofacies N* reappears for 5 m and then is followed by *Lithofacies O* (10 m thick) characterized by medium-grained biocalcarenites arranged in lenticular bodies, with breccias rich in large fossils (including discocyclines), grouped in lenses. We recognized nummulites (up to 4.5 cm in diameter) and discocyclines (up to 2.0 cm in diameter) grouped in lenses of centimetric to decimetric sizes. In the next 10 m, *Lithofacies N* is associated to *Lithofacies P*, consisting of homogeneous reddish marls with planktonic foraminifers indicative of a relative deepening. Upwards there follows *Lithofacies Q* (15 m thick), characterized by lenticular bodies of poorly stratified brecciated biocalcarenite bodies, which are rich in ostreids (5–10 cm in size), nummulites, discocyclines, assilines, annelids and lamellibranchs. Upwards, *Lithofacies O + Q* and *N* (40 m thick) and again the just described *Lithofacies O* appear between two semicovered intervals, for a total thickness of 30 m. The succession of Log 3 continues with *Lithofacies R* (10 m thick) consisting of well-cemented biocalcarenites (fine- to medium-grained, with larger foraminifera) containing globular nummulites (*N. perforatus*) and other flat forms, encrusting foraminifers and elongated alveolines. Breccias with fossiliferous intraclasts also occur. This lithofacies is followed by a new interval of *Lithofacies* N (5 m thick) and a new interval of *Lithofacies* R (5 m thick). After another interval of *Lithofacies N* (5 m thick) the succession ends with *Lithofacies S* (16 m thick), which is constituted by bioclastic limestones with small nummulites, ostreids and echinoderms.

In the stratigraphic section 3, six main microfacies (*Mf2*, *Mf3*, *Mf4*, *Mf5 Mf6*, *Mf7*) repeated several times and at different levels of the succession, and described afterwards, have been recognized.

4.1.4. Stratigraphic section 4 (Cánovas)

This stratigraphic section (Sierra Espuña Basin, Log. 4, 440 m thick) comprises the upper portion of the Malvariche Fm for a thickness of 340 m and the lower portion of the Cánovas Fm for a thickness of 100 m. In these two formations, different lithofacies have been recognized (Fig. 5 and Table 1). The age of the analyzed succession extends from middle Lutetian (SBZ15) to the Priabonian (SBZ19). The late middle Lutetian (SBZ15) was dated (Martín-Martín et al., 1997a, 1997b) with the LBF assemblage consisting of *N. aff. millecaput*, *N. aff. deshayesi*, *N. aff. tavertetensis*, *N. discorbinus*, *N.lorioli*, *N. beaumonti*, and *A exponens* (Fig. 4). The LBF assemblage consisting of *Alveolina gr. fragilis*, *N. aff. deshayesi*, *N. herbi*, *N. deshayesi*, *N. praepuschi*, *N. discorbinus*, *N. aff. biarritzensis*, *N. maximus*, *N. beaumonti*, and *A exponens* (Fig. 4) allowed to date the late middle Lutetian (SBZ16) (Martín-Martín et al., 1997a, 1997b). The LBF assemblage consisting of *Orbitolites complanatus*, *Alveolina gr. fragilis*, *N. aff. biarritzensis*, *N. maximus*, *N. perforatus*, *N. praegarnieri*, *N. beaumonti*, *N. hottingeri*, *A exponens*, *Discocyclina pratti pratti* and *Asterocyclina stellata stellata* (Fig. 4) allowed to date the early Bartonian (SBZ17) (Martín-Martín et al., 1997a, 1997b). Finally, the late Bartonian (SBZ18) was dated (Martín-Martín et al., 1997a, 1997b) with the LBF assemblage consisting of *N. praegarnieri*, *N. biedai*, *N. striatus* and *D. augustae augustae* (Fig. 4). The lower portion of this formation comprises *Lithofacies T* (50 m thick), which is characterized by unstratified brownish silty marls with planktonic foraminifers, colonial and solitary corals, large and flat nummulites, discocyclines, lamellibranchs, gastropods (e.g. turritellids); the fossils are oriented to delineate a pseudo-lamination. After an alternance of the previously described *Lithofacies* Q, T, Q for 75 m of thickness, there is *Lithofacies U* constituted by poorly stratified fine-grained bioclastic limestones (50 m thick) with corals, ostreids, gastropods (e.g. turritellids). The size of the fossils is much larger than the size of the other grains of the limestones. The Malvariche Fm ends with a new alternance of *Lithofacies Q, T + N, U, T, U* for a total thickness of 155 m.

After the last *Lithofacies U* of the Malvariche Fm, the succession passes to the upper Cánovas Fm (late Bartonian/SBZ18 to Priabonian/SBZ19). This formation was analyzed for the first 100 m, where three different lithofacies are recognized. The lower *Lithofacies Z* (thickness 40 m, including a 20 m thick semicovered interval) consists of fossiliferous marls and sands rich in assilines. Upwards there are 30 m of *Lithofacies W* characterized by brownish silty-marls with discocyclines (indicative of a deeper environment than the assilines according to

Table 2
Mf1 to *Mf8* description with the relative abundance of components, and depositional environment interpretation. Studied samples and fossil content (common, abundant, present and/or rare) are also shown.

Microfacies	Samples	Description	Fossils and non-skeletal grains common and/or abundant*	Fossils and non-skeletal grains present and/or rare	Depositional environment
Mf1	1 to 5, 9 to 10	Coralgal rhodolith packstone with hyaline LBF	Crustose coralline algae (*Sporolithon*, *Lithoporella*)*; *Solenomeris* macroids*, *Nummulites**, *Discocyclina**, *Asterocyclina**, hyaline encrusters (acervulinids, planorbulinids, homotrematids), rotaliids, haddonids; vinculariform bryozoans; annelids (*Ditrupa*); echinoid debris	*Alveolina*, *Aktinocyclina*, asterigerinids, discorbids, planktic foraminifers, miliolids, textulariids, hooked acervulinids; geniculate coralline algae	Proximal middle ramp LBF accumulations (nummulitids) Mesophotic environment
Mf2	6 to 8, 13, 14, 16 to 20, 22, 23, 27, 28, 30, 31, 33, 34, 40 to 42, 52 to 54	Hyaline LBF biocalcarenitic packstone	*Nummulites**, *Discocyclina**, *Asterocyclina**, pellets*, *Amphistegina*; rotaliids; hooked acervulinids; *Fabiania cassis;* solitary corals; pelecypods; annelids (*Ditrupa*); echinoid debris	*Alveolina*, *Assilina*, and operculiniform *Assilina*, *Aktinocyclina*, asterigerinids, discorbids, planktic foraminifers, miliolids, textulariids, geniculate coralline algae; bryozoan remains	Proximal middle ramp LBF accumulations (nummulitids) Mesophotic environment
Mf3	11, 12, 15, 21	Wackestone calcisiltite with gastropods	Gastropods, ostracods, small bivalves	Unspecific rotaliids	Inner ramp lagoon Euphotic upper subtidal environment
Mf4	26, 29, 32, 37, 39, 49, 51, 59, 60	Silty-marl wackestone with planktic foraminifers	Planktic and hyaline small benthic foraminifers (bolivinids); ostracods; mollusks	Miliolids, unspecific rotaliids	Outer ramp lacking LBF Oligophotic environment
Mf5	24, 36, 38	Quartzarenitic packstone with porcelaneous LBF	*Alveolina**, *Orbitolites**, discorbids*, pellets*, *Nummulites*, miliolids, rotaliids, hyaline encrusters (hooked acervulinids, planorbulinids, homotrematids), *Fabiania cassis*, rotaliids; dasyclades; geniculate coralline algae; pelecypods and gastropods; annelids (*Ditrupa*); echinoid debris	*Amphistegina*, asterigerinids, *Sphaerogypsina*, textulariids, haddonids, planktic foraminifers; bryozoan remains, lithoclasts	Inner ramp Sea grass Euphotic subtidal environment
Mf6	25	*Solenomeris* framestone	*Solenomeris**, haddonids	Discorbids, undeterminate rotaliids; corals; dasyclade and crustose coralline debris	Inner ramp Euphotic lower subtidal environment
Mf7	35	Acervulinid bindstone in quartzarenitic matrix	Acervulinid (*Solenomeris-Acervulina*)-planorbulinid macroids*, pellets*, *Solenomeris* fragments, hooked acervulinids, flat *Nummulites*, rotaliids, textulariids; geniculate coralline algae; echinoid debris; annelid worm tubes (*Ditrupa*)	Miliolids, *Sphaerogypsina*, *Amphistegina;* dasyclades; bryozoan fragments	Inner ramp Euphotic lower subtidal environment
Mf8	43 to 48, 50, 55 to 58	Silty marl packstone with hyaline LBF and solitary corals	*Discocyclina**, *Asterocyclina**, *Assilina**, *Nummulites**, solitary corals*, operculiniform *Assilina*, *Amphistegina*, planktic foraminifers; mollusks (turritellid gastropods, pectinids); echinoid debris	*Sphaerogypsina*; annelids; bryozoans	Distal middle ramp LBF accumulations (ortophrag-minids) Mesophotic environment

Hottinger, 1997); occasional metric calcarenite beds with discocyclines and occasional operculiniform assilines. The succession ends with *Lithofacies Y* (30 m thick) consisting in unstratified brownish to pinkish silty marls, with planktonic foraminifers and characterized by the absence of larger foraminifera.

In the stratigraphic section 4, mainly three microfacies (*Mf2*, *Mf4*, *Mf8*) are repeated several times and at different levels of the succession and will described afterwards.

In general, the litho- and biostratigraphic data indicate that the passage from Cuisian to early Lutetian (Espuña Fm) occurs in sedimentary continuity and transitional lithologies. On the contrary, an unconformity, observed in field, marks the contact between the Espuña Fm and the Malvariche Fm at the early-middle Lutetian boundary. This unconformity is considered a minor one since although it is recognized also in Logs 1 to 3, it does not have an associated biostratigraphic gap. The contact Malvariche/Cánovas Fms, corresponding to the early-late Bartonian, is transitional. The studied stratigraphic sections thus represent a complete or almost uninterrupted succession of the middle Eocene, from the SBZ13 to the SBZ18 and also of the underlying (late Cuisian/SBZ12) and overlying (Priabonian/SBZ19) stratigraphic intervals (Serra-Kiel et al., 1998a).

4.2. Microfacies description

On the basis of the fossiliferous assemblage, texture, and fabric, eight microfacies (*Mf1* to *Mf8*) have been recognized and named according to the first appearance in the analyzed stratigraphic sections (Table 2; Figs. 6 to 7A,B).

4.2.1. Microfacies of stratigraphic section 1 (Castillo de Mula)

4.2.1.1. Mf1 - coralgal rhodolith packstone with hyaline LBF (Table 2; Figs. 6F and 7A). This microfacies, poorly to moderately sorted, presents a floatstone to packstone texture with abundant crustose coralline algae (*Sporolithon*) in small- to medium-sized free warty to lumpy rhodoliths (ϕ: 3–10 mm) (15–20%) wrapped by the hyaline encrusting foraminifer *Acervulina linearis* and the agglutinate *Haddonia*, sometimes growing around bioclastic components such as bryozoans. Tests of *Nummulites* (20–25%), *Discocyclina* (10–15%) and *Asterocyclina* (10–15%) are also abundant. Frequently *Nummulites* tests make up the core of multilayered red algae encrusting successions (Type 2 of Nebelsick and Bassi, 2000) with alternating layers of *Lithothamnion* and *Lithoporella* thalli, acervulinids (*Solenomeris*, *Acervulina linearis*), planorbulinids, homotrematids (*Mniacina multiformis*), isolate discorbids and annelid worm tubes. Likewise, medium to large *Solenomeris* macroids (ϕ: >10 mm) (20–25%) in encrusting successions with hyaline foraminifer encrusters *Acervulina linearis* or *Miniacina* sp., agglutinate encruster *Haddonia heissigi* (1–2%), discorbids and annelids (*Ditrupa*) (2–3%) are also abundant. Common components distributed in the carbonate matrix are represented by rotaliids (*Gyroidinella laevis*, *Redmondina garganica*, *Neorotalia litothamnica*) (5%), bryozoans (5%), annelids, echinoid debris (2–3%) and remains of bivalves (ostreids) (2–3%). Other

components such as *Amphistegina*, *Sphaerogypsina*, asterigerinids, textularids, dasycladales and geniculate coralline algae can be observed occasionally. This microfacies is present only in this stratigraphic section with a thickness of about 45 m corresponding to the lithofacies M6, M7 and M9 (Fig. 5).

4.2.1.2. Mf2 - hyaline LBF biocalcarenitic packstone (Table 2; Figs. 6E and 7A). This facies, poorly to moderately sorted, is constituted mainly by abundant tests of *Nummulites* (30–35%), *Discocyclina-Asterocyclina* (5–10%) and numerous pellets (5–10%). Other common components are *Amphistegina* (2–3%), rotaliids (*Gyroidinella laevis*, *Carpenteria* sp., *Neorotalia* sp.) (5%), solitary corals (5–10%), undeterminate hook-like forms of acervulinids (5%), cymbaloporid *Fabiania cassis* (5%), geniculate coralline algae fragments (2%), pelecypods (2–5%) and echinoid debris (5%). Tests of *Alveolina*, *Assilina*, operculiniform *Assilina*, *Aktinocyclina*, asterigerinids, discorbids, planktic foraminifers, miliolids, textularids, valvulinids, *Acervulina linearis*, unspecific planorbulinids, bryozoan and annelid (*Ditrupa*) remains appear occasionally in the matrix. This microfacies is present in sections 1 to 3 with a total thickness of more than 485 m, and corresponds to the lithofacies M8, I, I1, I2, O, Q and R (Fig. 5).

4.2.2. Microfacies of stratigraphic section 2 (Prado Mayor)

4.2.2.1. Mf3 - wackestone calcisiltite with gastropods (Table 2; Figs. 6A and 7A). This microfacies is composed of calcareous fine-grained components in a wackestone texture that contains a low diversity biogenic assemblage constituted by abundant thin-walled ostracods (2–5%) and small bivalves (2–5%), and common ceritid gastropod shells (10–15%). Low abundant undeterminate rotaliids (2–3%) are also present. This microfacies is present in the stratigraphic sections 2 and 3 with a thickness of about 460 m and corresponds to the lithofacies G, H and H1–3 (Fig. 5).

4.2.3. Microfacies of stratigraphic section 3 (Malvariche)

4.2.3.1. Mf4 - silty-marly wackestone with planktic foraminifers (Table 2; Figs. 6H and 7B). The main components are planktic (5–10%) and hyaline small benthic foraminifers (bolivinids) (5–10%), common fine-walled ostracod (1–2%) and small mollusk shells (2–3%), rare miliolids and unspecified rotaliids. This microfacies, which is moderately sorted, is very common in stratigraphic sections 3 and 4 with a total thickness of about 275 m, corresponding to the lithofacies N, P, T, Z and Y (Fig. 5).

4.2.3.2. Mf5 – porcelaneous larger benthic foraminifer (LBF) quartzarenitic packstone (Table 2; Figs. 6B and 7B). This poorly- to moderately-sorted microfacies is made up of a fine- to medium-grained quartzarenite showing a main fossil association constituted by abundant *Alveolina* (10–15%), *Orbitolites* (10–15%) and discorbid tests (2–3%), peloids of unknown origin (5–7%), and an encrusting foraminifer assemblage composed by acervulinids (*Solenomeris ogormani*, *Acervulina linearis* and other undeterminate hook-like forms) (5–15%), planorbulinids (*Planorbulina* aff. *uva*, *P.* cf. *cretae*), homotrematids (*Miniacina* sp.) and *Fabiania cassis* (3–5%). Common to abundant tests of *Nummulites* (5–10%), miliolids (2–3%), rotaliids (*Gyroidinella laevis*, *Carpenteria* sp., *Neorotalia* sp.) (5%), dasyclade (1–2%) and geniculate coralline algae (2–5%), mollusk remains (pelecypods, gastropods) (2–5%), encrusting annelids (*Ditrupa*) (2–3%) and echinoid debris (5%) are also present. Other minor components are *Amphistegina*, asterigerinids, *Sphaerogypsina*, textulariids, agglutinate encrusting foraminifers (*Haddonia heissigi*), planktic foraminifers, bryozoan remains and lithoclasts. This microfacies is only present in this stratigraphic section with a thickness of about 65 m and corresponds to the lithofacies M and R *p.p.* (Fig. 5).

4.2.3.3. Mf6 - Solenomeris framestone (Table 2; Figs. 6C and 7B). This microfacies shows abundant *Solenomeris* growths (50–70%) encrusted by common agglutinate haddonid foraminifers (*Haddonia heissigi*) (10–15%). Other minor components dispersed in the matrix are discorbids (2–3%), undeterminate rotaliids (2–3%), corals (sometimes as nucleus of *Solenomeris* growths) (15–20%), dasycladales (2–3%) and crustose coralline algal debris (5%). This microfacies is only present in this stratigraphic section with a thickness of about 30 m and correspond to the lithofacies M *p.p.* (Fig. 5).

4.2.3.4. Mf7 - acervulinid macroids in quartzarenitic matrix (Table 2; Figs. 6D and 7B). This poorly- to moderately-sorted microfacies shows a floatstone to packstone texture mainly constituted by rounded acervulinid macroids and hyaline LBF tests within a well-sorted quartzarenitic matrix. Macroids (ϕ: 5.0–8.0 mm) are composed by encrusting acervulinids (*Solenomeris ogormani*, *Acervulina linearis*) (20–25%) and planorbulinids (*Planorbulina* aff. *uva*, *P.* sp.) (5–10%). Also unidentified hook-like acervulinid forms (*?Pseudogypsina* sp.) (10–15%) and peloids of unknown origin (5–10%) are a very abundant component. Fragmented *Solenomeris* (5%), flat *Nummulites* (5–10%), rotaliids (*Gyroidinella laevis*, *Neorotalia* sp.) (5%), textulariids (2–3%), geniculate coralline algae (5%), bivalve remains (ostreids) (2–3%), echinoid debris (5%) and annelid worm tubes (*Ditrupa*) (2–3%) are a common component interspersed in the matrix. Occasionally, tests of *Sphaerogypsina*, *Amphistegina*, miliolids, dasycladales and bryozoan fragments can be observed. This microfacies is present only in this stratigraphic section with a thickness of about 5 m and corresponds to the lithofacies R *p.p.* (Fig. 5).

4.2.4. Microfacies of stratigraphic section 4 (Cánovas)

4.2.4.1. Mf8 - silty marly packstone with hyaline LBF and azooxanthellate-like corals (Table 2; Figs. 6G and 7B). This moderately sorted microfacies presents a texture where macrofossils are mainly represented by LBF tests and solitary azooxanthellate-like corals (10–15%). These corals are shaped like a regular cone (cerioid-trocoid morphology), some of them flatted laterally (cupulate-flabellate morphology) which are up to 4 cm in both diameter and height, and showing regular radial septae. The assemblage of LBF is constituted by abundant to very abundant *Discocyclina-Asterocyclina* (25–30%) and *Nummulites* (10–15%). Also operculiniform *Assilina* (5–10%), *Assilina* (5%) and *Amphistegina* (5%), planktic foraminifers (2–3%), mollusks (turritellid gastropods, pectinid bivalves) (5–10%) and echinoids (5%) are a common component. Occasionally *Sphaerogypsina*, annelids, and bryozoans can appear. This microfacies is only present in this stratigrahic section with an elevate thickness of more than 285 m corresponding to the lithofacies T, Q, U and W (Fig. 5).

5. Discussion

5.1. Litho- and biofacies interpretation

In this section a paleoenvironmental interpretation will be provided based on the main litho- and microfacies characteristics. The marine inner to outer ramp paleoenvironments can be interpreted from proximal to distal areas as follows (Fig. 8):

5.1.1. Inner ramp

5.1.1.1. Mf3 - wackestone calcisiltite with gastropods. This microfacies is recognized in the Prado Mayor and Malvariche stratigraphic sections (Tables 1, 2). The lithofacies association mainly consists of micritic limestones and silty-sandy pelites with occasional quartzose arenites. This lithofacies from the Valdelaparra Fm shows low diversity of biogenic assemblage. It comprises abundant thin-walled ostracods, small bivalves and ceritid gastropods suggesting lagoonal deposits. The early Eocene

portion of this stratigraphic formation was interpreted by Martín-Martín et al. (2020c) as the transition to shallow-marine (subtidal) environments in euphotic conditions. The presence of non-evergreen vegetation (possibly seasonal vegetation, likely algal) is not ruled out given the numerous small herbivorous-like gastropods observed (Beavington-Penney et al., 2004; Reich et al., 2015).

5.1.1.2. Mf5 – porcelaneous LBF quartzarenitic packstone. This microfacies is recognized in the Malvariche stratigraphic section (Tables 1, 2) and comprises alternating limestones and sandy-pelites, and storm brecciated limestone beds and biocalcarenites. The dominant bioassociation is constituted by *Orbitolites*, hooked acervulinids (due to encrustation on organisms with a blade or cylindrical morphology, such as leaves of marine phanerogams, vegetative structures of algae or branchy colonies of bryozoa), miliolids, discorbids and often associated encruster annelids (*Ditrupa*), suggesting the presence of seagrass meadows (Beavington-Penney et al., 2004; Reich et al., 2015; Tomás et al., 2016; Tomassetti et al., 2016). *Orbitolites*, like the current *Sorites*, is often considered a temporary to permanent attached foraminifera, which is a common component associated to blades and rhizomes of marine phanerogams but also to smaller algae (Langer, 1993; Mateu-Vicens et al., 2014). Discorbids, with the flat-convex or concave-convex morphology of their tests, are another group of foraminifers habitually related to an epiphytic way of life (Murray, 2006). Small miliolids and textulariids, as permanently motile and grazing foraminifers, are often associated to sediment-rich plant microhabitats such as rhizomes of both phanerogams and algae (Langer, 1993; Murray, 2006; Mateu-Vicens et al., 2014). The presence of terrigenous quartz grains can be explained by the baffling-trapping effect of the vegetation, and *Alveolina*, as one of the main components of this facies, would be the result of reworking and trapping by currents from neighboring inner ramp areas without vegetation. The joint presence of other components such as dasycladales and geniculate coralline algae, mollusks and echinoids is also compatible with euphotic subtidal seagrass environments in the inner ramp.

5.1.1.3. Mf6 - Solenomeris framestone. This microfacies is shown in the Malvariche stratigraphic section (Tables 1, 2), which is mainly represented by limestones (brecciated limestones related to storms in the upper portion), alternating with Nummulite-rich sandy-pelites. The microfacies is mainly made up of a bioconstruction of the encrusting acervulinid foraminifer *Solenomeris* covering a coral substrate. Autochtonous *Solenomeris* bioconstructions have been interpreted by several authors as marine bioherms in conditions of light reduction in deeper environments than coral reefs (Perrin, 1992; Bosellini and Papazzoni, 2003). This fact could indicate a deepening of the depositional environment after a first phase of coral colonization, or alternatively an increase in the turbidity of the waters due to terrigenous input, with a parallel increase in the trophic conditions of the environment that would result in a reduction of light intensity. The infilling matrix in this biogenic structure is mainly composed by discorbids, rotaliids, dasyclade green algae, bryozoa and crustose coralline algae suggesting mesotrophic conditions in low to medium energy environments. The deduced light reduction would indicate that this environment could correspond to the lower euphotic inner ramp in the transition to the mesophotic middle ramp.

5.1.1.4. Mf7 - acervulinid bindstone in quartzarenitic matrix. This microfacies appears in the Malvariche stratigraphic section (Tables 1, 2) and consists of biocalcarenites, sometimes showing storm brecciated structures. The microfacies is characterized by the presence of rounded acervulinid macroids, which require for their formation the presence of some bottom currents. The main components (abundant peloids, hook-like acervulinids, rotaliids, textulariids and geniculate coralline algal fragments) suggest euphotic inner ramp environments, with the presence of a seagrass meadow. The important quartzarenitic component of the matrix comes from baffling and trapping by vegetation of the terrigenous material, generating a mixing siliciclastic-carbonate sedimentary facies (Mount, 1984; Mateu-Vicens et al., 2012a). The input of terrigenous depends on the rainfall in the hinterland and on sea-level

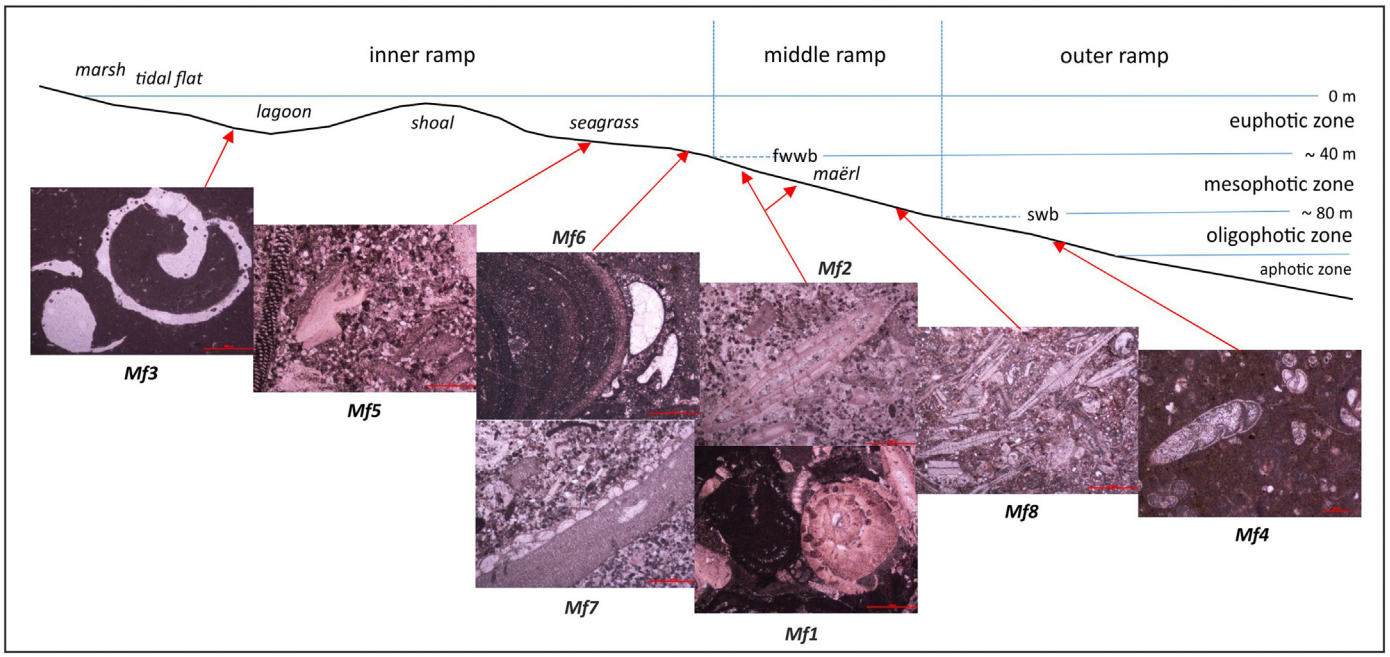

Fig. 8. Environmental microfacies distribution for the Middle Eocene marine Depositional Sequence 2 (Malvariche and Cánovas fms) in Sierra Espuña, arranged from proximal to distal depositional environments: *Mf3*, Inner ramp lagoon, upper subtidal environment; *Mf5*, Inner ramp seagrass, euphotic subtidal environment; *Mf6 - Mf7*, Inner ramp, euphotic lower subtidal environment; *Mf2*, Proximal middle ramp LBF accumulations (nummulitids), mesophotic environment; *Mf1*, Proximal middle ramp maërl, mesophotic environment; *Mf8*, Distal middle ramp LBF accumulations (orthophragminids), mesophotic environment; *Mf4*, Outer ramp lacking LBF, oligophotic environment. Ramp subdivision is based on Burchette and Wright (1992), and photic zones are analogous to those described by Pomar et al. (2017), with a 'mesophotic zone' comprised between lower limit of occurrence of marine vegetation and the storm wave base (swb).

changes. This period correspond with a relative sea-level fall and with a warm climate (LLTM) probably with high rainfall. Both factors agree with the input of terrigenous sediments derived from erosion in the emerged lands.

5.1.2. Middle ramp

5.1.2.1. Mf1 – coralgal rhodolith packstone with hyaline LBF. This microfacies is in the Castillo de Mula stratigraphic section (Tables 1, 2). The prevalent associated lithotypes is related to storm levels and emersion moments. They consist of amalgamated biocalcarenites, sandy marls with occasional Fe—Mn nodules (related to emersion moments), chaotic intraformational conglomerates, calcareous blocks sometimes including decametric ocraceous nodular discontinuous levels and storm discontinuous beds of biocalcarenites. The microfacies, with dominant red algae and *Solenomeris*, is attributed to a maërl environment in the upper portion of a middle ramp. It consists of a foraminiferal-coralline algal facies with free-living warty rhodoliths on a coarse-grained mobile substrate. The great abundance of parautochtonous *Solenomeris* macroids suggests reduced light conditions (Perrin, 1992; Bosellini and Papazzoni, 2003). Also the abundant presence of hyaline-LBF tests of *Nummulites* and orthophragminids (*Discocyclina* and *Asterocyclina*) imply initial oligotrophic and mesophotic conditions for this deposit (Hottinger, 1997; Geel, 2000), which could undergo a change to mesotrophic conditions as indicated by the important presence of red algae and encruster foraminifers overlaying the LBF.

5.1.2.2. Mf2 - hyaline LBF biocalcarenitic packstone. This microfacies was recognized in the Castillo de Mula and Malvariche stratigraphic sections (Tables 1, 2). These lithofacies consist of biocalcarenites and bioclastic limestones (sometimes in lenticular bodies with a brecciated structure), alternating with pelitic-sandy levels (sometimes with nummulites), intraformational conglomerates related to storms (coming from the inner ramp) and sandy marls.

The dominance of hyaline-LBF accumulations of *Nummulites* and orthophragminids (*Discocyclina*, *Asterocyclina*) tests indicates oligotrophic and mesophotic conditions in a marine middle ramp (Hottinger, 1997; Geel, 2000). Notwithstanding abundant peloids and a considerable presence of a shallow-marine assemblage consisting of hook-like acervulinids possibly associated to seagrass environments (Tomás et al., 2016), geniculate coralline algal fragments and isolate alveolinids characteristic of an inner ramp suggest a contribution of reworked elements from shallower areas during some energetic high energy events such as storms.

5.1.2.3. Mf8 - silty marl packstone with hyaline LBF and solitary corals. This microfacies is represented in the Malvariche stratigraphic section (Tables 1, 2), which mainly consists of silty-marls and occasional calcarenites. The biofacies assemblage of hyaline LBF, mainly composed by orthophragminids (*Discocyclina*, *Asterocyclina*) and *Nummulites*, has been regularly associated to oligotrophic and mesophotic environments (Hottinger, 1997; Geel, 2000; Racey, 2001) corresponding to the lower part of the middle ramp. The additional presence of solitary corals suggests also deeper marine conditions (Cairns, 2007; Kiessling and Kocsis, 2015) near the transition to the oligophotic outer ramp but with a noticeable nutrient content, which contrasts with the oligotrophic habitats of LBF. It could be explained from sudden nutrient supply events in a mainly oligotrophic environment, which would drive to solitary corals thrive in these depositional settings (Kiessling and Kocsis, 2015). These authors indicate that in the non-photosymbiotic group nutrition comes exclusively from heterotrophic feeding, whereas the photosymbiotic group achieves a good part of its nutrition from algae hosted in the coral's tissue. The middle-late Eocene transition was a warm period with an increase in rainfall on the continent and in sedimentary contributions from there. In such conditions, Kiessling and Kocsis (2015) attributed the migration of solitary corals to deep environments in non-reef habitats and on siliciclastic substrates, and their consequent development to increased nutrient concentrations in deeper waters.

5.1.3. Outer ramp

5.1.3.1. Mf4 - silty-marly wackestone with planktic foraminifers. This microfacies was mainly observed in the Castillo de Mula, Malvariche and Cánovas stratigraphic sections (Tables 1, 2). It consists of unstratified silty-marls and homogeneous silty-sandy pelites. The low diversity of this facies, which is made up mainly of abundant planktic foraminifers in a calcareous muddy sediment suggests open marine conditions in oligophotic outer ramp environments, located distally to the hyaline-LBF accumulation belts, as in the models proposed by several authors (Buxton and Pedley, 1989; Burchette and Wright, 1992; Flügel, 2010). Furthermore, the dominant presence of small benthic bolivinids indicates outer shelf and upper bathyal settings (Bandy, 1960), and their reduced surface sculpture denotes low oxygen concentrations in bottom sediments (Lutze, 1964; Obiosio, 2013).

5.2. Paleoenvironmental evolution

All the above reported description indicates that the Espuña, Valdelaparra, Malvariche and Canovas Fms deposited during a fluctuating trend of relative sea-level changes during the middle Eocene. The shallow-marine environments show an inner ramp (lagoon or seagrass, with a certain energy to roll the rhodoliths, both in euphotic upper subtidal environments), evolving upward to middle ramp (Maërl in mesophotic environments) and later to a distal middle ramp (LBF-orthophragminid accumulations in mesophotic environments) and finally to oligophotic outer ramp environments (circalittoral). In the study area, inner ramps usually show mesotrophic conditions, middle ramps settings mainly show oligotrophic conditions, and outer ramps show oligotrophic to mesotrophic conditions. A representation is shown in Fig. 9, where a synthetic stratigraphic section with the relative sea-level changes, terrigenous-nutrients inputs, environments, trophic and photic conditions, and main biotic assemblages of the study area are correlated. This figure allows giving more details on the evolution as follows.

In detail, during the early Lutetian inner ramp (lagoon) mesotrophic to eutrophic conditions arranged in a regressive trend took place (Fig. 9). This was followed by two transgressive sequences with terrigenous-nutrients inputs where all the ramps environments alternated and mesotrophic evolved upwards to oligo-mesotrophic conditions during the early middle Lutetian (Fig. 9). During the late middle Lutetian, two transgressive followed by a regressive sequence accounted, where the middle and outer ramp environments and mesotrophic and oligotrophic conditions alternated (Fig. 9). This was followed by two transgressive sequences with terrigenous-nutrients inputs where the inner (seagrass) and the outer ramp environments alternated and oligo-mesotrophic and oligotrophic conditions also alternated during the late Lutetian (Fig. 9). The early Bartonian is also characterized by two transgressive sequences representing the outer and the middle ramp with oligotrophic to highly oligotrophic conditions (Fig. 9). The studied succession ends with the late Bartonian to Priabonian transgressive sequence, where the middle and outer ramp is represented with mesotrophic, oligo-mesotrophic and oligotrophic conditions alternate (Fig. 9).

The fossiliferous assemblage described in the middle Eocene deposits of Sierra Espuña shows a mixing of mainly photozoan (coralline/green algae, LBF and azooxanthellate-like corals) and heterotrophic components (small benthic and planktic foraminifers, ostracods, mollusks, echinoids, bryozoans, annelids and solitary corals). The photozoan association indicates variable photic (euphotic to oligophotic) conditions in oligotrophic marine warm-water environments at low to middle latitudes. Heterotrophic components, traditionally ubiquitous, dominate

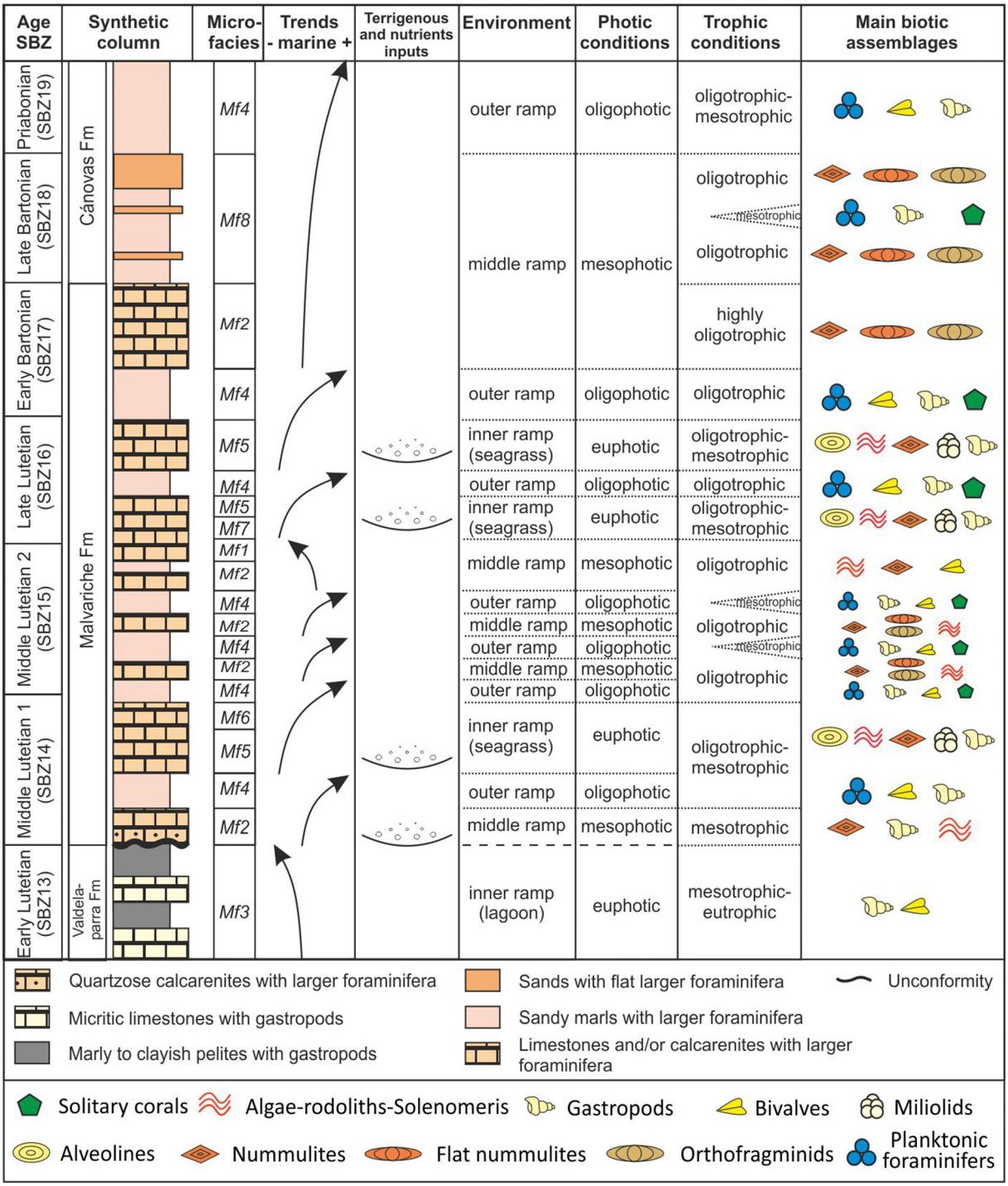

Fig. 9. Synthetic column from the middle Eocene from the Sierra Espuña-Mula area with correlation with the transgressive-regressive trends, terrigenous-nutrients inputs, sedimentary environments, photic and trophic conditions, and main biotic assemblages.

mesotrophic to eutrophic marine habitats of any depth. They can occur associated to the photozoan assemblage or as unique association. Their presence sharing habitat with LBF suggests some local mesotrophic conditions for recycling organic matter from the soft sea-bottom by burrowing activity in mainly oligotrophic settings (Hottinger, 1983); however, they can also occur as a unique association indicating steps of increase in the nutrient availability. The biogenic assemblage of middle Eocene deposits of this area can be assigned to the 'subtropical' Heterozoan+ association (James, 1997), or to the 'foralgal facies' (Wilson and Vecsei, 2005), which indicate low-latitude deposits dominated by non-framework building, light-dependent biota such perforate LBF, coralline algae and sometimes green algae. These environments correspond to warm-water marine environments. The presence of a complete depth-related LBF assemblage, from euphotic to oligophotic conditions, suggests a progressive marine ramp model under essentially oligotrophic conditions eventually influenced by detrital sediment supply from continent currents that increase the nutrient content of marine waters. In such conditions, the presence of upwelling currents cannot be discarded in moments of coral appearance (Kiessling and Kocsis, 2015). Analogous depositional models have been described in the literature by Buxton and Pedley (1989), Racey (2001), and Beavington-Penney et al. (2006) for Middle Eocene deposits of the Seeb Fm of Northern Oman,

and for the same time interval in the Central Pyrenees by Payros et al. (2010) or Silva-Casal (2017). A paleogeographic 3D representation is shown in Fig. 10, where paleoenvironments are displayed laterally for the whole Middle Eocene according to the Walter Law rules.

5.3. Middle Eocene paleoenvironmental evolution of other sectors of the Tethyan domain

The middle Eocene paleoenvironmental evolution of the studied area is compared with other Tethyan sectors, starting from the Betic and Rifian sectors, in order to obtain general constraints for the evolution of the Western Tethys platforms during the considered time span.

5.3.1. Betic and Rifian sectors

Middle Eocene shallow-marine successions are mainly described in Malaguide and Prebetic units of the Betic Chain. A paleogeographic sketch of middle Eocene Tethys is shown in Fig. 11, where the paleo-position of studied sector is marked with the number (1) and the compared areas are reported with the numbers 2 to 13. The Sierra Espuña succession shows similarities with Prebetic ones (2). This unit is widely represented in the Alicante region (Geel et al., 1998; Geel, 2000; Höntzsch et al., 2013), and locally in Albacete and Murcia areas (Jerez, 1981; Kenter et al., 1990; Vera, 2000). The Prebetic platforms show highly varied paleogene sediments: shallow-marine deposits are mainly distributed in the northern sector of the region, passing to deep deposits in the southern one. The more complete middle Eocene shallow-marine deposits have been described by Geel (2000) in the Ibi section (Alicante region). These deposits are arranged into five shallowing-upwards sequences composed by mainly hyaline LBF-rich limestones (nummulites, assilines and discocyclines), deposited in an inner to middle marine ramp. According to the former author, these sequences should be controlled by tectonics and relative sea-level changes. A tectonic tilting in the region at the end of this period would cause an emersion and erosion of the highest parts of the general stratigraphic succession, marking the end of the middle Eocene sedimentation (Kenter et al., 1990; Geel et al., 1998). Coeval shallow-marine deposits are also found in the Malaguide units, around the city of Malaga where they are represented by alveoline-limestone olistostromic blocks in a marine slope environment (Serrano et al., 1995), and in the Velez Rubio corridor in Almería, where they show similar features to those of Sierra Espuña area but are reduced in extension and thickness (Jabaloy Sánchez et al., 2019).

In the Internal Unit of the Rif Chain (Ghomarides) in the NE Morocco at the surroundings of the city of Tetouan, a fairly complete Paleocene to Middle Eocene shallow-marine succession showing a clearly deepening trend is reported (Maaté et al., 2000). The Ghomarides (3) have a paleogeographic origin close to the Malaguide units of the Betic Cordillera (Martín-Martín et al., 2020c) in the westernmost Tethys. Middle Eocene deposits are represented by micritic limestones with a diverse and abundant assemblage of LBF (alveolins, nummulites, assilins and discocyclins), where the presence of *N. boussaci* indicates a middle Lutetian 1 (SBZ 14) age. Z-corals were not found by these authors. The sequence ends with planktonic foraminifera-rich marls and silts of an imprecise middle Eocene age, probably corresponding to the middle Lutetian-Bartonian interval.

5.3.2. Other Tethyan sectors

Shallow-marine middle Eocene environments are represented at a wide range of paleolatitudes ranging from 40°N to 40°S (Philip et al.,

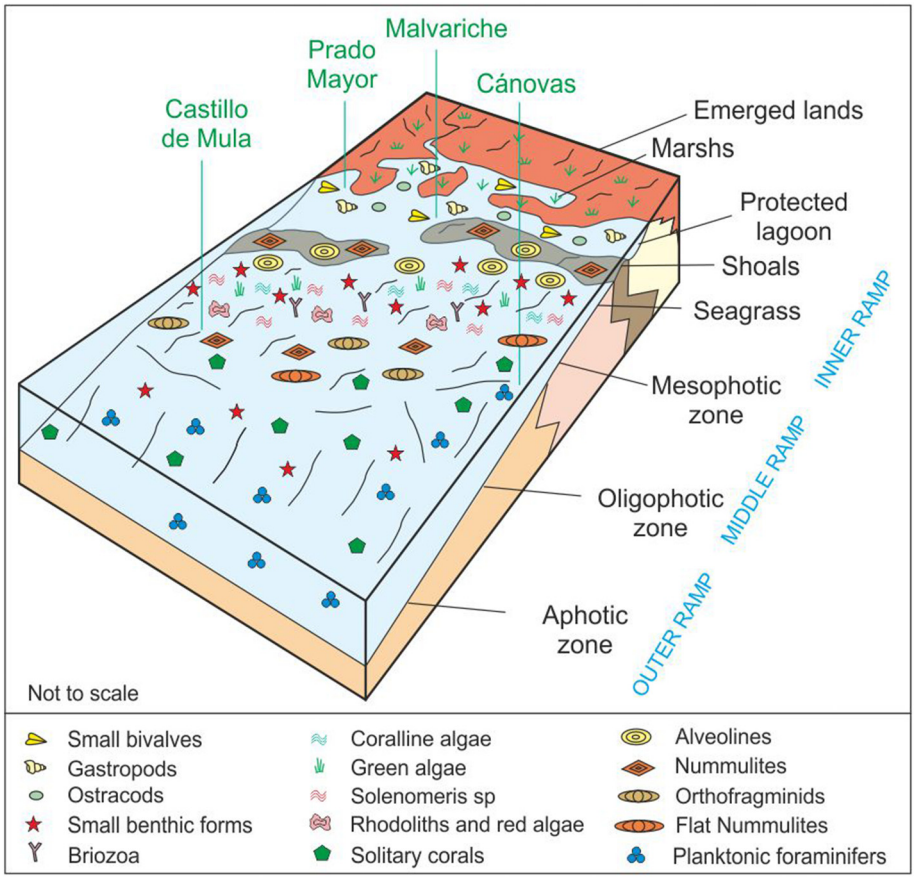

Fig. 10. Paleogeographic and paleoenvironmental 3D sketch of the Sierra Espuña-Mula basin area.

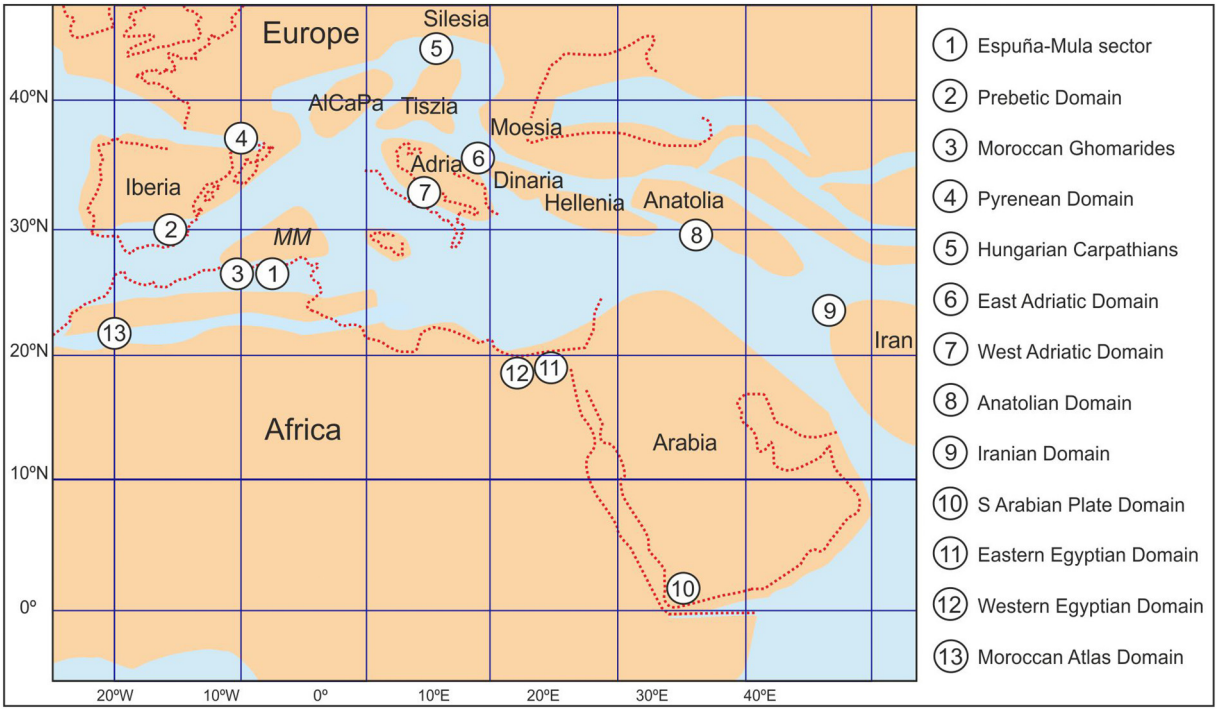

Fig. 11. Paleogeographic map near the Cretaceous/Cenozoic boundary (about 70 Ma) showing the location of the study area and the compared sectors (after Scheibner and Speijer, 2008; Martín-Martín et al., 2020b; modified).

2013). In the circum-Tethyan area, these environments are well developed along its northern margin from the Pyrenean region to the Tibetan area across the Alps, Adriatic, Appenines, Carpathian, Great Caucasus, Hellenian, Anatolian and Indian domains (Fig. 11). In the southern circum-Tethyan margin, these platforms extend between Morocco and Oman across Tunisian, Libyan, Egyptian and Arabian platforms. In general, sediments are represented by wide LBF-rich belts, extended in homoclinal ramps ranging from euphotic to oligophotic conditions, with interspersed seagrass and coralline algal mäerl environments, and sporadic development of coral patch-reefs.

- Pyrenees (4). Middle Eocene shallow-marine sediments of Lutetian age are widely spread in the southern passive margin of the Central Pyrenean basin (External Sierras) and are represented by several shallowing-upwards limestone sequences with abundant and diverse LBF assemblages (Martín-Martín et al., 2001; Barnolas et al., 2004; Rodríguez-Pintó et al., 2012). Scattered corals in the Early Lutetian (Rodríguez-Pintó et al., 2012), coral-mounds in the late middle Lutetian (Poblet et al., 1998; Pomar et al., 2017) and local small coral biostromes/bioherms of late Lutetian age (Morsilli et al., 2012; Mateu-Vicens et al., 2012b; Pomar et al., 2017) are present. In the southeastern Pyrenean foreland basin, this interval shows four nummulitid-rich transgressive-regressive sedimentary cycles in Lutetian sediments, and other two ones in Bartonian deposits (Taberner et al., 1999; Serra-Kiel et al., 2003a). Some isolated coral patch-reefs are recorded in the late Lutetian of the Vic area (Taberner and Bosence, 1985). The early Bartonian cycle (SBZ 17) is characterized by well-developed Nummulite-banks and isolated coral patch-reefs (Serra-Kiel et al., 2003b), and the upper one (SBZ 18) ends with a well-developed coral reef interval (Taberner et al., 1999; Romero et al., 2002).
- Hungarian (5) Paleogene basin. The middle Eocene shallow-marine sedimentation starts with terrigenous coastal deposits of the early Lutetian (*Nummulites laevigatus* level) topped by unconformable middle Lutetian-early Bartonian carbonates with LBF (*Assilina spira* marls and *Nummulites perforatus-N. millecaput-maximus groups* limestone) and some rare coral reefs. The deposition is arranged in a deepening sequence that ends with glauconite- and planktic foramifers-rich calcareous marls (Báldi-Beke and Báldi, 1991; Kazmer et al., 2003).
- East Adriatic domain (6). This region comprises a major part of the entire carbonate succession cropping out in the Croatian part of the Karst Dinarides (Vlahovic et al., 2005). The middle Eocene shallow-marine sedimentation of this area is especially developed in the Istrian area and is represented mainly by wide LBF-dominated belts with the only presence of ahermatypic corals in late Lutetian deposits (Cosovic et al., 2004). However, Maticec et al. (1996) cite the presence in W Istria of corals, in a Middle Eocene transgressive sequence constituted by foraminiferal and coralgal packstones. Likewise, data from wells drilled in middle Eocene platform carbonates in the northern and middle Adriatic point to the presence of coral debris and isolated corals within transgressive LBF-rich limestones deposited on shallow-marine platforms, and on marginal platform buildups (Kovacic, 1997). Finally, the presence of corals is also reported for shallow-marine limestones of early Lutetian reworked in younger slope deposits of the W Herzegovina platforms (Dragicevic et al., 1992).
- West Adriatic domain (7). The middle Eocene shallow-marine sedimentation is represented mainly in the Apulian Platform outcrops of the Maiella Mountains (Vecsei et al., 1998) and the Gargano Promontory, where these deposits include nummulite and discocycline calcarenites with small coral patch-reefs (Bosellini et al., 1999; Morsilli et al., 2017).
- Anatolian domain in Turkey (8). In the northern Turkish Thrace Basin, the shallow-marine middle Eocene sedimentation is characterized by LBF-rich carbonates, which alternate with coral-dominated levels that developed notorius patch-reefs in late Lutetian and early Bartonian deposits, but especially at the late Bartonian-Priabonian transition (Özcan et al., 2010).
- Iran (9). Data on middle Eocene shallow-marine sediments from the northern Iran Alborz region report a deepening sequence extending from late Lutetian?-early Bartonian limestones, with nummulites, corals and coralline red algae (SBZ 16?-17), to late Bartonian marly

limestones, with abundant nummulites, orthophragmines and coralline red algae (SBZ 18) (Hadi et al., 2019).

- South Arabian Plate (10). The middle Eocene sequence in Yemen is represented by shaly lagoonal deposits (early Lutetian, SBZ 13) overlain by an inner to middle ramp carbonate sedimentation (middle-late Lutetian) with alveolines, orbitolites and nummulites. The uppermost nummulite-rich member (SBZ 17–18) contains abundant hermatypic corals, algae, and mollusks (Robinet et al., 2013; Serra-Kiel et al., 2016).
- Egypt. In the northern Egypt, the Bartonian deposits of the eastern sectors (11) are dominated by LBF-rich bioclastic and marly limestones that include coral-debris and dendroid coral patches (Tawfik et al., 2016). On the contrary, in the Western Desert (12) the presence of corals decreases and they are replaced by nummulite banks and bryozoan-mollusk facies. Similar facies are widely developed westwards in the rest of the northern African margin.
- Moroccan Atlas (13). Coeval sediments are also represented in the Atlas region, and are included in the so-called Subatlas Group (Herbig and Trappe, 1994), which integrates a latest Cretaceous to middle Eocene transgressive-regressive megacycle. This area is the closest to the Atlantic domain, and consists of a non-deformed pretectonic unit, deposited in an epicontinental sea that is characterized by peritidal and inner ramp sedimentation in eutrophic settings as indicated by the absence of LBF and corals. Also, a limestone bioclastic highly fossiliferous sequence is reported from the eastern Ouarzazate Basin, containing mollusks (oyster lumachelles), echinoids, green algae, small benthic foraminifers (miliolids, rotalids, discorbids) and ostracods (Herbig and Trappe, 1994; El Harfi et al., 2001). Locally, palynologic data suggest a mangrove environment, and likewise, the presence of selacean teeth, dominated by batoids, is characteristic of shallow-marine environments (Tabuce et al., 2005).

The above-mentioned occurrences suggest that during the middle Eocene coral-reef buildups (z-corals) were widespread on shallow-marine environments of the central and eastern Tethys Ocean, but these deposits are neither of great dimensions nor dominant, because of the much widespread presence of LBF. Only coral-reef patches are scattered on the broad LBF-rich belts developed in shallow-marine settings, especially with thermal events (LLTM and MECO; SBZ16–17). A general zonation of LFB and z-coral buildups was proposed by Pomar et al. (2017) and references therein (Fig. 12). Nevertheless, our study allows to concrete that these coral constructions are completely absent in the westernmost Tethys.

According to Adams et al. (1990) and Langer and Hottinger (2000), the LBF distribution is restricted to a worldwide climatic belt with temperatures above 15–20 °C and controlled by the extent of low-nutrient water masses. However, these authors also argue that the current areas of high LBF diversity coincide with regions of high sea-surface temperatures. Thus, the middle Eocene, as the peak for LBF diversity in the Tethys, reaches optimal conditions to make this group thrive in an intertropical belt with broad homoclinal ramps, developing new ecological niches to be colonized. In these conditions, z-corals were not very widespread, being only present as small patches scattered in various ramp environments, at several periods throughout the circum-Tethyan region. As a consequence, it is not possible to recognize a direct relationship with climate or ecological factors. For example, they are present in eastern Egypt but disappear westward in the remaining part of northern African Tethyan domains. This absence in the westernmost Tethys could be explained by the presence of nutrient-rich upwelling (Herbig, 1986; Herbig and Trappe, 1994; Scheibner and Speijer, 2008). LFB seem to be better adapted to such conditions than corals. In our oppinion, the particular paleogeography of the westernmost Tethys, with the proximity of a narrow and deep basin (as the MFB) connected to the Atlantic Ocean (Guerrera et al., 2021) could explain this absence of z-corals, and even the absence of LFB in the Atlas Moroccan zone.

5.4. LBF distribution, specific diversity and test size: ecological vs climate controls

The main environmental parameters that explain the widely presence of LBF in several time intervals are temperature and oligotrophy (Hottinger, 1983; Hallock, 1985, 2000). Thus, warming climate, the rainfall (including the influence in the terrigenous runoff), but also ocean circulation pattern, controlling the trophic conditions, could explain several questions regarding the morphological characters and sizes of tests, specific diversity and/or intraspecific variability, number of appearances and last occurrences of species in the circum-Tethyan LBF assemblage during the middle Eocene. We can highlight among others the following issues:

- Highest diversities of Tethyan LBF coincide with this period (Adams et al., 1990; Hallock et al., 1991; Brasier and Bosence, 1995; Whidden and Jones, 2012; Pomar et al., 2017). According to Hottinger (1983), they are well represented in peripheral Atlantic basins (Pyrenees) and especially in the northern Tethyan margin, from the Alps to Turkey, with low values in diversity in the northern African subprovince. In the Sierra Espuña area, the diversity is remarkable (Figs. 12 and 4) but without reaching the high values of the Pyrenean domain.
- Largest tests in dominant genera have been reported for this period: *Nummulites* in the late Lutetian and early Bartonian (Schaub, 1981; Ungaro, 1994; Brasier and Bosence, 1995), *Assilina* in the middle-late Lutetian (Schaub, 1981), and *Alveolina* from middle Lutetian to early Bartonian (SBZ 14–17; Hottinger and Drobne, 1988). For *Nummulites*, this fact occurs with the terminal species of every philetic group (i.e. *N. perforatus-N. biedai*, *N. puschi-N. brongniarti*, *N. millecaput-N. maximus*, *N. gizehensis*, *N. carteri*) (Schaub, 1981), which are characterized by a high intraspecific variability that in some cases can hinder the precision in the taxonomic determination. In the Sierra Espuña area, both *N. perforatus-N. biedai* and *N. puschi* or *N. millecaput-N. maximus* groups are well represented in late Lutetian (SBZ 16) and early Bartonian deposits (SBZ 17). So some giant forms of *N. maximus* have been observed in these sediments, with tests that can reach 10 cm in diameter. Furthermore, these species, although generally represented throughout the Tethys, are usually dominant in certain subprovinces: *N. perforatus-N.biedai*, *N. puschi-N. brongniarti* and *N. millecaput-N. maximus* groups in the peripheral Atlantic basins but also in the Malaguide Sierra Espuña area and on the northern margin of the circum-Tethyan area, *N. syrticus* and *N. gizehensis* in the North African domain, and *N. carteri* in the Indian subcontinent (Blondeau, 1972; Schaub, 1981). This suggests a certain provincialism among these faunas, as it happens in the Sierra Espuña area.
- Maximum specific diversity in *Alveolina* is observed in the early Eocene (Hottinger and Drobne, 1988; Serra-Kiel et al., 1998a), prior to maximum development in test size. Despite the sharp decline in diversity observed at the Ypresian-Lutetian boundary, a new diversification phase is observed in the Early Lutetian according to data of Serra-Kiel et al. (1998a), indicating the wide presence of ecologically stable inner ramp environments. Then, a widespread decline in diversity is observed through the middle Eocene, in negative correlation with the trend of alveolines to reach maximum sizes and elongation of their tests (Hottinger and Drobne, 1988; Brasier and Bosence, 1995). In the Sierra Espuña area, alveoline-rich inner ramp settings are mainly represented in the Malvariche section, during the late Lutetian and early Bartonian (Fig. 7b), by alveoline specimens of the *A. fragilis* group with very elongated, length tests. The last occurrence (LO) of alveoline in the study area (Fig. 12) takes place in the earliest Bartonian (SBZ17) slightly before to that proposed by Hottinger (1960, 1997) probably conditioned by the absence in this area of inner ramp realms in the late middle Eocene.
- Maximum specific diversities in nummulitids and orthophragminids are observed in the middle Lutetian (SBZ14–15), with values maintained during the late Lutetian-early Bartonian (SBZ16–17) (Schaub,

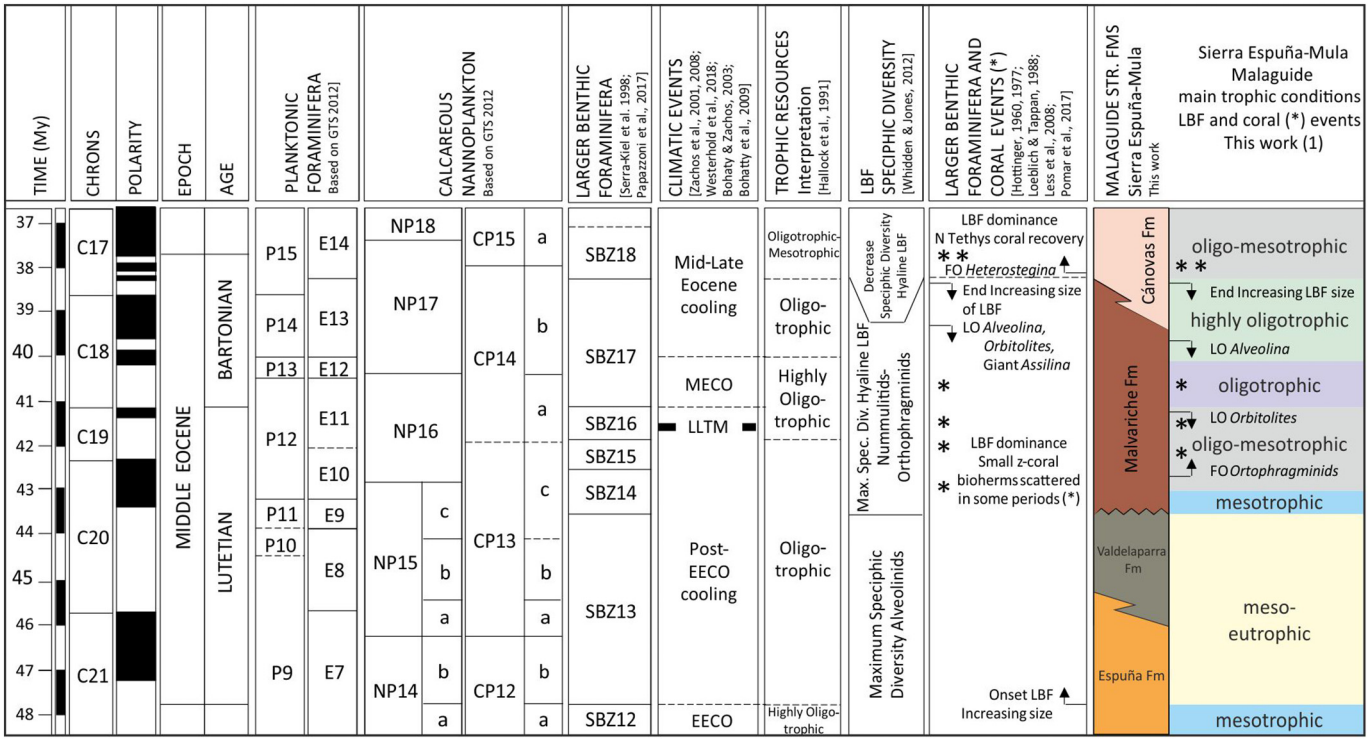

Fig. 12. Biochronostratigraphic chart with numerical time scale, magnetochrons, magnetic polarity, planktonic foraminifera and calcareous nannoplankton zones based on GTS 2012 (Gradstein and Ogg, 2012), correlated with shallow benthic zones (SBZ). Interpretations of main climatic events, trophic resources continuum, LBF specific diversity and coral events in the Tethyan domain are also represented. A synthetic column with the stratigraphic formations and the main trophic conditions and LBF and coral (*) events of the Sierra Espuña-Mula Basins are also included.

1981; Serra-Kiel et al., 1998a; Whidden and Jones, 2012; Pomar et al., 2017), to indicate widespread marine middle to outer ramp environments at this time span. On the other hand, maximum diversities in LBF are related to generalized oligotrophic to highly oligotrophic conditions (Brasier and Bosence, 1995), which denotes a marked environmental stability that favors the dominance of k-strategist communities (Hottinger, 1983). This has also led us to re-interpret data concerning the "Trophic Resources continuum" provided by Hallock et al. (1991) that considered the middle Eocene as a period of 'decreasing oligotrophic habitats'. According to systematic data of nummulitids from Serra-Kiel et al. (1998b) revised in this work (Fig. 4), this variation in specific diversity is well reflected in sediments of middle Lutetian age (SBZ 14–15) from the Sierra Espuña area. Here, the number of taxa recognized is relatively high (13 species), but it decreases in the late Lutetian (9 species), early Bartonian (7 species) and late Bartonian (3 species).

- Highest values on first occurrences (FO) in nummulitid and orthophragminid species (Fig. 12) are found in the middle Lutetian (mainly SBZ14), and they decrease abruptly in the late Lutetian-early Bartonian interval (SBZ16–17; Whidden and Jones, 2012; Pomar et al., 2017), coinciding with the above-mentioned provincialism of many of the species of nummulitids represented at this period and with hyperthermal events reported in literature (LLTM and MECO). According to the data of nummulitids recognized by Serra-Kiel et al. (1998b) in the Sierra Espuña area and revised in this work (Fig. 4), the number of FO of species with a well-recognized stratigraphic range has a low value, being 6 in the early-middle Lutetian (SBZ 14), 1 in the late middle Lutetian (SBZ 15), 4 in the late Lutetian (SBZ 16), 3 in the early Bartonian and 2 in the late Bartonian, in correspondence with the low specific diversity recognized in this area. According to Hottinger (1997), 'when the full specific diversity is reached, the communities start to diverge in separate faunal provinces', which is observed in this timespan. This evolutionary step, especially in large nummulitids can also be associated to the 'critical phase of the radiation interval' prior to the 'mass extinction interval' according to Brasier and Bosence (1995) that happens at the end of early Bartonian (SBZ 17). In the Sierra Espuña area the considered timespan is well represented, with a nummulitid assemblage mainly composed by species of *Nummulites perforatus*, *N. puschi-N. herbi* and *N. millecaput-maximus* groups. The late Lutetian is represented, respectively by *N. deshayesi*, *N. praepuschi-N. herbi* and *N. maximus*. On the other hand, the early Bartonian is mainly represented by *Assilina exponens*, *N. perforatus* and some small forms (*N. praegarnieri*, *N. hottingeri* and *N. beaumonti*). The base of the Cánovas Fm is represented in the type-section by *N. biedai*, *N. praegarnieri* and *N. striatus*, indicating the lowermost part of the late Bartonian (SBZ 18).

The importance of the early-late Bartonian boundary (SBZ17–18) should be emphasized as a critical scenario of biological change recognizable in all shallow-marine environments across the Tethys (Fig. 11) with the end of increasing of LBF size, which is also reflected in the Sierra Espuña Basin (Fig. 12):

- The end of increasing size of LBF tests, the LO of *Alveolina*, *Orbitolites* and giant *Assilina* s.s. (only "operculiniform *Assilina*" cross this threshold), and the first occurrence of the genre *Heterostegina* are noted (Loeblich and Tappan, 1987; Less et al., 2008).
- A noticeable reduction in specific diversity of hyaline LBF, mainly nummulitids and orthophragminids (Whidden and Jones, 2012), allowed to consider an oligotrophic to mesotrophic setting for the marine carbonate neritic environments of this interval, coinciding with the 'demise of k-strategists' according to the Trophic Resources continuum by Hallock et al. (1991) and with the end of the MECO climate event.
- The general dominance of LBF in shallow-marine environments of the Tethys decreases sharply through this boundary and a recovery

of the zooxanthellate corals is observed (not in our study area), with a gradual increase in size, number, and diversity of coral-buildup ecosystems, replacing LBF-dominated environments. This event will become especially effective from the late Eocene with decreasing global temperatures related to the formation of first glaciation on the Antarctic continent. A paleogeographic control does not seem the origin for this change since in the westernmost Tethys the MFB was not closed until the early Miocene (Guerrera et al., 2021). The increase in the presence of coral bioherms across this boundary is not reflected in the Sierra Espuña deposits due to the deepening-upwards sedimentary trend that during this period does not allow the development of shallowest marine facies in this area.

6. Conclusions

The middle Eocene period, as the peak for LBF diversity in the Tethys, indicates optimal conditions for thriving of this group in an intertropical belt with broad homoclinal shallow-marine ramps free to be colonized and to develop new ecological niches. Z-corals were much reduced through the circum-Tethyan region. A clear direct relationship to climate or ecological changes has not been recognized. Even, these are absent in the westernmost Tethys.

Nevertheless, both issues seem to be related to the increasing temperatures throughout this interval. Symbiont algae present in corals tend to disappear when a temperature threshold is exceeded, unlike those found in LBF, allowing these to thrive in warmer sea-waters. The conjunction of high temperatures and low nutrient content of ocean waters, as well as the available space on continental margins, all closely related to the high sea level conditions in this period. The sea-level rise propitiated a transgression allowing the extensive development of shallow-marine environments in the flooded areas. All the above give rise to the high specific diversity recorded in LBF during this timespan.

It is worth noting the differences in the fossiliferous assemblage of most marine platforms on the northern Tethyan margin with respect to those on the southern margin. In eastern Egypt, z-coral buildups are present but disappear in the rest of northern African Tethyan domains, west of the Central Egypt desert. In the Atlas region, not only corals are missing but also LBF, suggesting eutrophic conditions related to nutrient-rich upwelling areas making LFB life impossible (Herbig, 1986; Herbig and Trappe, 1994; Scheibner and Speijer, 2008).

The great specific diversity in LBF across the Pyrenean area and the northern Tethyan margin during middle Eocene is not reflected in the Sierra Espuña area. Others issues affecting the morphological characters and evolution of LBF as sizes of the tests, specific diversity and/or intraspecific variability, number of appearances and last occurrences of species in the circum-Tethyan LBF assemblage during this time, have been also revised in the LBF assemblage of the Sierra Espuña area. The presence of largest tests during the late Lutetian-early Bartonian interval has been evidenced for the genera *Alveolina*, with centimetric very elongated tests, but also for *Nummulites*, especially in the *N. millecaput-maximus* group, with tests that reach 10 cm in diameter, and in the *N. perforatus* group, parallel to an increase of intraspecific variability in these taxa. The loss of specific diversity along this period has also been observed in *Nummulites*, the best-represented generus, from the middle Lutetian (SBZ14–15) to the late Bartonian (SBZ18). The greatest number of first occurrences in nummulitid species (*Nummulites* and *Assilina*), as in the rest of the Tethys, is observed at the onset of the middle Lutetian and decreases progressively in the late Lutetian, and Bartonian, in correspondence with the decrease in specific diversity. All these data can be related to moments of increase in global temperatures coinciding with main warmer events through the middle Eocene (LLTM and MECO) and only secondarily to the nutrient content of marine waters.

Finally, the importance of the early-late Bartonian boundary (SBZ17–18) as a critical scenario of biological change recognizable across the shallow-marine environments must be highlighted. This scenario is also reflected in the Sierra Espuña Basin, with (i) the end of increasing size of LBF tests; (ii) the last occurrence of *Alveolina*, *Orbitolites* and giant *Assilina* and the FO of the genus *Heterostegina*; and (iii) a marked reduction in specific diversity of hyaline LBF (nummulitids and orthophragminids). This reduction can be explained by an increase of trophism in the shallow-marine waters, which led to a reduction in the prevalence of LBF and a recovery of the zooxanthellate corals, with a gradual increase in size, number, and diversity of coral bioherms, replacing LBF-rich belts.

Declaration of competing interest

The authors declare that they have no known competing financial interests or personal relationships that could have appeared to influence the work reported in this paper.

Acknowledgments

Research supported by: Research Project CGL2016-75679-P, Spanish Ministry of Education and Science; Research Groups and Projects of the Generalitat Valenciana, Alicante University (CTMA-IGA); University of Urbino “Carlo Bo”, Research Funds to F. Guerrera and M. Tramontana. The revisions performed by Prof. André Strasser and an annonymous reviewer are also acknowledged.

References

Adams, C.G., Lee, D.E., Rosen, B.R., 1990. Conflicting isotopic and biotic evidence for tropical seasurface temperatures during the Tertiary. Palaeogeography Palaeoclimatology Palaeoecology 77, 289–313.
Báldi-Beke, M., Báldi, T., 1991. Palaeobathymetry and palaeogeography of the Bakony Eocene Basin in western Hungary. Palaeogeography Palaeoclimatology Palaeoecology 88, 25–52.
Bandy, O.L., 1960. General correlation of foraminiferal structure with environment. 21st lntern.l Geol. Congress Proceedings, Norden 22, pp. 1–19.
Barnolas, A., Payros, A., Samsó, J.M., Serra-Kiel, J., Tosquella, J., 2004. La Cuenca surpirenaica desde el Ilerdiense medio al Priaboniense. In: Vera, J.A. (Ed.), Geología de España (SGE-IGME), pp. 313–320 Madrid.
Beavington-Penney, S.J., Wright, V.P., Woelkerling, W.J., 2004. Recognising macrophyte-vegetated environments in the rock record: a new criterion using ‘hooked’ forms of crustose coralline red algae. Sedimentary Geology 166, 1–9.
Beavington-Penney, S.J., Wright, V.P., Racey, A., 2006. The Middle Eocene Seeb Formation of Oman: an investigation of acyclicity, stratigraphic completeness, and accumulation rates in shallow marine carbonate settings. Journal of Sedimentary Research 76 (10), 1–25.
Blondeau, A., 1972. Les Nummulites. De l’Enseignement à la Recherche-Sciences de la Terre. Ed, Vuibert, Paris (254 pp.).
Bohaty, S.M., Zachos, J.C., 2003. Significant Southern Ocean warming event in the late middle Eocene. Geology 31 (11), 1017–1020.
Bosellini, F.R., Papazzoni, C.A., 2003. Palaeoecological significance of coral-encrusting foraminiferan associations: a case-study from the Upper Eocene of northern Italy. Acta Palaeontologica Polonica 48 (2), 279–292.
Bosellini, A., Morsilli, M., Neri, C., 1999. Long-term event stratigraphy of the Apulia Platform Margin (Upper Jurassic to Eocene, Gargano, Southern Italy). Journal of Sedimentary Research 69 (6), 1241–1252.
Brasier, M.D., Bosence, D.W.J., 1995. Fossil indicators of nutrient levels. 2: evolution and extinction in relation to oligotrophy. In: Alison, P.A. (Ed.), Marine Palaeoenvironmental Analysis From Fossils. 83. The Geological Society of London, spec. publ, pp. 133–150.
Burchette, T.P., Wright, V.P., 1992. Carbonate ramp depositional systems. Sedimentary Geology 79, 3–57.
Buxton, M.W.N., Pedley, H.M., 1989. Short Paper: a standardized model for Tethyan Tertiary carbonate ramps. Journal of the Geological Society of London 146, 746–748.
Cairns, S.D., 2007. Deep-water corals: an overview with special reference to diversity and distribution of deep-water scleractinian corals. Bulletin of Marine Science 81, 311–322.
Cosovic, V., Drobne, K., Moro, A., 2004. Paleoenvironmental model for Eocene foraminiferal limestones of the Adriatic carbonate platform (Istrian Peninsula). Facies 50, 61–75.
Doglioni, C., 1992. Main differences between thrust belts. Terra Nova 4, 152–164.
Dragicevic, I., Blaskovic, I., Tisljar, J., Benic, J., 1992. Stratigraphy of Paleogene Strata within the Mesihovina - Rakitno Area (Western Herzegovina). Geologia Croatica 45, 25–52.
Dunham, R.J., 1962. Classification of carbonate rocks according to depositional texture. American Association of Petroleum Geologists, Memoir 1, 108–121.
Edgar, K.M., Wilson, P.A., Sexton, P.F., Suganuma, Y., 2007. No extreme bipolar glaciation during the main Eocene calcite compensation shift. Nature 448 (7156), 908–911.
El Harfi, A., Lang, J., Salomon, J., Chellai, E.H., 2001. Cenozoic sedimentary dynamics of the Ouarzazate foreland basin (Central High Atlas Mountains, Morocco). Internat. J. of Earth Sciences 90, 393–411.

Flügel, E., 2010. Microfacies of carbonate rocks. Analysis, Interpretation and Application. Springer (976 pp.).
Geel, T., 2000. Recognition of stratigraphic sequences in carbonate platform and slope deposits: empirical models based on microfacies analysis of Paleogene deposits in southeastern Spain. Palaeogeography, Palaeoclimatology, Palaeoecology 155, 211–238.
Geel, T., Roep, T.B., Vail, P.R., Van Hinte, J.E., 1998. Eocene tectono-sedimentary patterns in the Alicante region (Southeastern Spain). In: Hardenbol, J., Thierry, J., Farley, M.B., Jacquin, T., De Graciansky, P.R., Vail, P.R. (Eds.), Mesozoic and Cenozoic Sequence Chronostratigraphic Framework of European Basins. SEPM spec. publ 60, pp. 289–302.
Glynn, P., 1996. Coral reef bleaching: facts, hypotheses and implications. Global Change Biology 2, 495–510.
Gradstein, F.M., Ogg, J.G., 2012. Chapter 2 - the chronostratigraphic scale. In: Gradstein, F. M., Ogg, J.G., Schmitz, M.D., Ogg, G.M. (Eds.), The Geologic Time Scale. Elsevier, pp. 31–42.
Guerrera, F., Martín-Martín, M., 2014. Geodynamic events reconstructed in the Betic, Maghrebian and Apennine chains (central-western Tethys). Bulletin de la Société Géologique de France 185 (5), 329–341.
Guerrera, F., Martín-Martín, M., Perrone, V., Tramontana, M., 2005. Tectono-sedimentary evolution of the southern branch of the western Tethys (Magrebian Flysch basin and Lucanian ocean). Terra Nova 17, 358–367.
Guerrera, F., Mancheño, M.A., Martín-Martín, M., Raffaelli, G., Rodríguez-Estrella, T., Serrano, F., 2014. Paleogene evolution of the External Betic Zone and geodynamic implications. Geologica Acta 12 (3), 171–192.
Guerrera, F., Martín-Martín, M., Tramontana, M., 2021. Evolutionary geological models of the central-western peri-Mediterranean chains: a review. International Geology Review 63 (1), 65–86. https://doi.org/10.1080/00206814.2019.1706056.
Hadi, M., Less, G., Vahidinia, M., 2019. Eocene larger benthic foraminifera (alveolinids, nummulitids, and orthophragmines) from the eastern Alborz region (NE Iran): taxonomy and biostratigraphy implications. Revue de Micropaleontologie 63, 65–84.
Hallock, P., 1985. Why are larger Foraminifera large? Paleobiology 11, 195–208.
Hallock, P., 2000. Symbiont-bearing foraminifera: harbingers of global change? Micropaleontology 46 (1) (95-10).
Hallock, P., Premoli Silva, I., Boersma, A., 1991. Similarities between planktonic and larger foraminiferal evolutionary trends through Paleogene paleoceanographic changes. Palaeogeography, Palaeoclimatology, Palaeoecology 83, 49–64.
Herbig, H.G., 1986. Lithostratigraphisch-fazielle Untersuchungen im marinen Alttertiär südlich des zentralen Hohen Atlas (Marokko), Berliner geowiss. Abh. (A) 66, 343–380.
Herbig, H.G., Trappe, J., 1994. Stratigraphy of the Subatlas Group (Maastrichtian-Middle Eocene, Morocco). Newsletters on Stratigraphy 30 (3), 125–165.
Höntzsch, S., Scheibner, C., Brock, J.P., Kuss, J., 2013. Circum-Tethyan carbonate platform evolution during the Palaeogene: the Prebetic platform as a test for climatically controlled facies shifts. Turkish Journal of Earth Sciences 22, 891–918.
Hottinger, L., 1960. Recherches sur les Alvéolines du Paléocène et de l'Éocène. Mémoires Suisses de Paléontologie, Basel, pp. 1–243.
Hottinger, L., 1983. Processes determining the distribution of larger foraminifera in space and time. Utrecht Micropaleontology Bulletin 30, 239–253.
Hottinger, L., 1997. Shallow benthic foraminiferal assemblages as signals for depth of their deposition and their limitations. Bulletin de la Société Géologique de France 168 (4), 491–505.
Hottinger, L., Drobne, K., 1988. Tertiary Alveolinids: problems linked to the conception of species: Revue de Paléobiologie, Benthos '86. Spec. Vol. 2 pp. 665–681.
Jabaloy Sánchez, A., Martín-Algarra, A., Padrón-Navarta, J.A., Martín-Martín, M., Gómez-Pugnaire, M.T., López Sánchez-Vizcaíno, V., Garrido, C., J., 2019. Lithological successions of the internal zones and Flysch Trough Units of the Betic Chain. The Geology of Iberia (A Geodynamic Approach), pp. 377–432 (chapt. 8).
James, N.P., 1997. The cool-water carbonate depositional realm. In: James, N.P., Clarke, J.A. D. (Eds.), Cool-water Carbonates, SEPM Spec. Publ. 56, pp. 1–22.
Jerez, F., 1981. Propuesta de un nuevo modelo tectónico general para las Cordilleras Béticas. Boletín Geológico y Minero XCII-I 1–18.
Kazmer, R., Dunkl, I., Frisch, W., Kuhlemann, J., Ozsvart, P., 2003. The Palaeogene forearc basin of the Eastern Alps and Western Carpathians: subduction erosion and basin evolution. Journal of the Geological Society, London 160, 413–428.
Kennett, J.P., Stott, L.D., 1991. Abrupt deep-sea warming, palaeoceanographic changes and benthic extinctions at the end of the Palaeocene. Nature 353 (6341), 225–229.
Kenter, J.A.M., Reymer, J.J.G., van der Straaten, H.C., Peper, T., 1990. Facies patterns and subsidence history of the Jumilla-Cieza region (southeastern Spain). Sedimentary Geology 67, 263–280.
Kiessling, W., Kocsis, A., 2015. Biodiversity dynamics and environmental occupancy of fossil azooxanthellate and zooxanthellate scleractinian corals. Paleobiology https://doi.org/10.1017/pab.2015.6.
Kovacic, V.T., 1997. The development of the Eocene platform carbonates from wells in the Middle Adriatic Off-Shore Area. Croatia. Geol. Croat. 50 (1), 33–48.
Langer, M.R., 1993. Epiphytic Foraminifera. Marine Micropaleontology 20, 235–265.
Langer, M.R., Hottinger, L., 2000. Biogeography of selected larger foraminifera. Micropaleontology 46 (Suppl. 1), 105–126.
Less, G., Ozcan, E., Papazzoni, C.A., Stockar, R., 2008. The middle to late Eocene evolution of nummulitid foraminifer Heterostegina in the Western Tethys. Acta Palaeontologica Polonica 53 (2), 317–350.
Loeblich, A.R., Tappan, H.P., 1987. Foraminiferal genera and their classification. Van Nostrand Reinhold Company 2 (970 pp.).
Lutze, G.F., 1964. Statistical investigations on the variability of *Bolivina argéntea*, Cushman. Cushman Foundation for Foraminiferal Research Contributio 15, 105–116.
Maaté, A., Martín-Algarra, A., Martín-Martín, M., Serra-Kiel, J., 2000. Nouvelles données sur le Paléocène-Éocène des zones internes bético-rifaines. Geobios 33 (4), 409–418.
Martín-Algarra, A., 1987. Evolución geologíca alpina del con- tacto entre las Zonas Internas y las Zonas Externas de la Cordillera Bética. Univ. Granada, Spain (Ph Tesis; 1187 pp.).
Martín-Martín, M., 1996. El Terciario del Dominio Maláguide en Sierra Espuña (Cordillera Bética oriental, SE de España). Univ. Granada, Spain (PhD Thesis, 299 pp.).
Martín-Martín, M., Robles-Marín, M., 2020. Alternative methods for calculating compaction in sedimentary basins. Marine and Petroleum Geology 113, 104132.
Martín-Martín, M., Martín-Algarra, A., Serra-Kiel, J., 1997a. El Terciario del Dominio Maláguide en Sierra Espuña (Prov. De Murcia, SE de España). Revista de la Sociedad Geológica de España 10 (3–4), 265–280.
Martín-Martín, M., El Mamoune, B., Martín-Algarra, A., Martín-Pérez, J.A., Serra-Kiel, J., 1997b. Timing of deformation in the Malaguide of the Sierra Espuña (Southeastern Spain). Geodynamic evolution f the Internal Betic Zone. Geologie en Mijnbow 75 (4), 309–316.
Martín-Martín, M., Serra-Kiel, J., El Mamoune, B., Martín-Algarra, A., Serrano, F., 1998. The Paleocene of the Eastern Malaguides (Betic Cordillera, Spain): stratigraphy and paleogeography. Comptes Rendus Geosciences 326, 35–41.
Martín-Martín, M., Rey, J., Alcalá-García, F.J., Tosquella, J., Deramond, J., Lara-Corona, E., Duranthon, F., Antoine, P.O., 2001. Tectonic controls of the deposits of a foreland basin: an example from the Eocene Corbières-Minervois basin, France. Basin Research 13, 419–433.
Martín-Martín, M., Martín-Rojas, I., Caracuel, J.E., Estévez-Rubio, A., Martín-Algarra, A., Sandoval, J., 2006. Tectonic framework and extensional pattern of the Malaguide Complex from Sierra Espuña (Internal Betiz Zone) during Jurassic-Cretaceous: implications for the Westernmost Tethys geodynamic evolution. International Journal of Earth Sciences 95, 815–826.
Martín-Martín, M., Guerrera, F., Tramontana, M., 2020a. Geodynamic implications of the latest Chattian-Langhian central-western peri-Mediterranean volcano-sedimentary event: a review. The Journal of Geology 128, 29–43.
Martín-Martín, M., Guerrera, F., Miclaus, C., Tramontana, M., 2020b. Similar Oligo-Miocene tectono-sedimentary evolution of the Paratethyan branches represented by the Moldavidian Basin and Maghrebian Flysch Basin. Sedimentary Geology 396, 105548.
Martín-Martín, M., Guerrera, F., Tosquella, J., Tramontana, M., 2020c. Paleocene-Lower Eocene carbonate platforms of westernmost Tethys. Sedimentary Geology 404, 105674.
Mateu-Vicens, G., Brandano, M., Gaglianone, G., Baldassarre, A., 2012a. Seagrass meadow sedimentary facies in a mixed siliciclastic-carbonate temperate system in the Tyrrhenian Sea (Pontinian Islands, Western Mediterranean). Journal of Sedimentary Research 82, 451–463.
Mateu-Vicens, G., Pomar, L., Ferràndez-Cañadell, C., 2012b. Nummulitic banks in the upper Lutetian 'Buil level', Ainsa Basin, South Central Pyrenean Zone: the impact of internal waves. Sedimentology 59, 527–552.
Mateu-Vicens, G., Khokhlova, A., Sebastián-Pastor, T., 2014. Epiphytic foraminiferal indices as bioindicators in mediterranean seagrass. Journal of Foraminiferal Research 44 (3), 325–339.
Maticec, D., Vlahovic, I., Velic, I., Tisljar, J., 1996. Eocene limestones overlying Lower Cretaceous deposits of Western Istria (Croatia): did some parts of present Istria Form Land during the Cretaceous? Geologica Croatica 49 (1), 117–127.
Morsilli, M., Bosellini, F., Pomar, L., Hallock, P., Aurell, M., Papazzoni, C.A., 2012. Mesophotic coral buildups in a prodelta setting (Late Eocene, southern Pyrenees, Spain): a mixed carbonate-siliciclastic system. Sedimentology 59, 766–794.
Morsilli, M., Hairabian, A., Borgomano, J., Nardon, S., Adams, E.W., Bracco Gartner, G.L., 2017. The Apulia Carbonate Platform-Gargano Promontory, Italy (Upper Jurassic-Eocene). AAPG Bulletin 101 (4), 523–531.
Mount, J.F., 1984. Mixing of siliciclastic and carbonate sediments in shallow shelf environments. Geology 112, 432–435.
Murray, J.W., 2006. Ecology and Applications of Benthic Foraminifera. Cambridge University Press (426 pp.).
Nebelsick, J.H., Bassi, D., 2000. Diversity, growth forms and taphonomy: key factors controlling the fabric of coralline algae dominated shelf carbonates. In: Insalaco, E., Skelton, P.W., Palmer, T.J. (Eds.), Carbonate Platform Systems: Components and Interactions. 178. Geological Society London, spec. publ., pp. 89–107.
Obiosio, E.O., 2013. Biostratigraphy and Paleoenvironment of *Bolivina* Fauna from the Niger Delta, Nigeria. Earth Science Research 2 (2), 80–92.
Özcan, E., Less, G., Okay, A.I., Báldi-Beke, M., Kollanyi, K., Yılmaz, I.O., 2010. Stratigraphy and Larger Foraminifera of the Eocene Shallow-Marine and Olistostromal Units of the Southern Part of the Th race Basin, NW Turkey. Turkish Journal of Earth Sciences 19, 27–77.
Papazzoni, C., Cosovic, V., Briguglio, A., Drobne, K., 2017. Towards a calibrated Larger Foraminifera biostratigraphic zonation: celebrating 18 years of the application of Shallow Benthic Zones. Palaios 32, 1–5.
Payros, A., Pujalte, V., Tosquella, J., Orue-Etxebarria, X., 2010. The Eocene storm-dominated foralgal ramp of the western Pyrenees (Urbasa–Andia Formation): an analogue of future shallow-marine carbonate systems? Sedimentary Geology 228, 184–204.
Perrin, C., 1992. Signification ecologique des foraminifères acervulinidés et leur role dans la formation de facies récifaux et organogènes depuis le Paléocène. Geobios 25 (6), 725–751.
Perrin, C., Kiessling, W., 2010. Latitudinal trends in Cenozoic reef patterns and their relationship to climate. In: Mutti, M., Piller, W., Betzler, C. (Eds.), Carbonate Systems During the Oligocene-Miocene Climatic Transition. IAS spe. publ. 42. Wiley-Blackwell, pp. 17–34.
Philip, J., Masse, J.-P., Camoin, G., 2013. Tethyan carbonate platforms. In: Nairn, A.E.M., Ricou, L.-E., Vrielynck, B., Dercourt, J. (Eds.), The Ocean Basins and Margins, Ch. 4A. Springer Science and Business Media, LLC, pp. 239–265.

Poblet, J., Muñoz, J.A., Travé, A., Serra-Kiel, J., 1998. Quantifying the kinematics of detachment folds using three-dimensional geometry: application to the Mediano anticline (Pyrenees, Spain). GSA Bulletin 110, 111–125.
Pomar, L., 2001. Types of carbonate platforms: a genetic approach. Basin Research 13, 313–334.
Pomar, L., Baceta, J.I., Hallock, P., Mateu-Vicens, G., Basso, D., 2017. Reef building and carbonate production modes in the west-central Tethys during the Cenozoic. Marine and Petroleum Geology 83, 261–304.
Prazeres, M., Roberts, T.E., Pandolfi, J.M., 2017. Variation in sensitivity of large benthic Foraminifera to the combined effects of ocean warming and local impacts. Sci Rep. 7, 45227.
Racey, A., 2001. A review of eocene nummulite accumulations: structure, formation and reservoir potential. Journal of Petroleum Geology 24 (1), 79–100.
Reich, S., Di Martino, E., Todd, J.A., Wesselingh, F.P., Renema, W., 2015. Indirect paleoseagrass indicators (IPSIs): a review. Earth-Science Reviews 143, 161–186.
Rivero-Cuesta, L., Westerhold, T., Agnini, C., Dallanave, E., Wilkens, R.H., Alegret, L., 2019. Paleoenvironmental changes at ODP Site 702 (South Atlantic): anatomy of the Middle Eocene Climatic Optimum. Paleoceanography and Paleoclimatology 34 (12), 2047–2066.
Rivero-Cuesta, L., Westerhold, T., Alegret, L., 2020. The Late Lutetian Thermal Maximum (middle Eocene): first record of deep-sea benthic foraminiferal response. Palaeogeography, Palaeoclimatology, Palaeoecology 545, 1–11.
Robinet, J., Razin, P., Serra-Kiel, J., Gallardo-García, A., Leroy, S., Roger, G., Grelaud, C., 2013. The Paleogene pre-rift to syn-rift succession in the Dhofar margin (northeastern Gulf of Aden): stratigraphy and depositional environments. Tectonophysics 607, 1–16.
Rodríguez-Pintó, A., Pueyo, E.L., Serra-Kiel, J., Samsó, J.M., Barnolas, A., Pocoví, A., 2012. Lutetian magnetostratigraphic calibration of larger foraminifera zonation (SBZ) in the southern Pyrenees: the Isuela section. Palaeogeography, Palaeoclimatology, Palaeoecology 333-334, 107–120.
Romero, J., Caus, E., Rosell, J., 2002. A model for the palaeoenvironmental distribution of larger foraminifera based on late Middle Eocene deposits on the margin of the South Pyrenean basin (NE Spain). Palaeogeography, Palaeoclimatology, Palaeoecology 179, 43–56.
Sarkar, S., 2017. Microfacies analysis of larger benthic foraminifera-dominated Middle Eocene carbonates: a palaeoenvironmental case study from Meghalaya, N-E India (Eastern Tethys). Arab Journal Geosciences 10, 121.
Schaub, H., 1981. Nummulites et Assilines de la Tethys paleogene. Taxinomie, phylogenese et biostratigraphie. Memoirs Schweiz de Paleontologie 104–106 (1 238).
Scheibner, C., Speijer, R.P., 2008. Decline of coral reefs during late Paleocene to early Eocene global warming. Earth-Science Reviews 3, 19–26.
Scheibner, C., Speijer, R.P., Marzouk, A.M., 2005. Turnover of larger foraminifera during the Paleocene-Eocene Thermal Maximum and paleoclimatic control on the evolution of platform ecosystems. Geology 33 (6), 493–496.
Serra-Kiel, J., Hottinger, L., Caus, E., Drobne, K., Ferràndez, C., Jauhri, A.K., Less, G., Pavlovec, R., Pignatti, J., Samsó, J.M., Schaub, H., Sirel, E., Strougo, A., Tambareau, Y., Tosquella, J., Zakrevskaya, E., 1998a. Larger foraminiferal biostratigraphy of the Thetian Paleocene and Eocene. Bull. Soc. Géol. Fr. 169 (2), 281–299.
Serra-Kiel, J., Martín-Martín, M., El Mamoune, B., Martín-Algarra, A., Martín-Pérez, J.A., Tosquella, J., Ferràndez-Cañadell, C., Serrano, F., 1998b. Biostratigraphy and lithostratigraphy of the Paleogene of the Sierra Espuña area (oriental Betic Cordillera, SE Spain). Geologica Acta 32 (1–3), 161–189.
Serra-Kiel, J., Travé, A., Mató, E., Saula, E., Ferràndez-Cañadell, C., Busquets, P., Tosquella, J., Vergés, J., 2003a. Marine and transitional Middle/Upper Eocene units of the southeastern Pyrenean foreland basin (NE Spain). Geologica Acta 1 (2), 177–200.
Serra-Kiel, J., Mató, E., Saula, E., Travé, A., Ferràndez-Cañadell, C., Busquets, P., Samsó, J.M., Tosquella, J., Barnolas, A., Álvarez-Pérez, G., Franquès, J., Romero, J., 2003b. An inventory of the marine and transitional Middle/Upper Eocene deposits of the Southeastern Pyrenean Foreland Basin (NE Spain). Geologica Acta 1 (2), 201–229.
Serra-Kiel, J., Gallardo-Garcia, A., Razin, Ph., Robinet, J., Roger, J., Grelaud, C., Leroy, S., Robin, C., 2016. Middle Eocene-Early Miocene larger foraminifera from Dhofar (Oman) and Socotra Island (Yemen). Arabian Journal of Geosciences 9 (5), 1–95.
Serrano, F., Sanz de Galdeano, C., Delgado, F., López-Garrido, A.C., Martín-Algarra, A., 1995. The Mesozoic-Cenozoic of the Malaguide Complex in the Málaga area: a Paleogene olistostrome-type chaotic complex (Betic Cordillera, Spain). Geologie en Mijnbouw 74, 105–116.
Sexton, P.F., Norris, R.D., Wilson, P.A., Pälike, H., Westerhold, T., Röhl, U., Bolton, C.T., Gibbs, S., 2011. Eocene global warming events driven by ventilation of oceanic dissolved organic carbon. Nature 471 (7338), 349–352.
Silva-Casal, R., 2017. Las plataformas carbonatadas del Eoceno medio de la cuenca de Jaca-Pamplona (Formación Guara, Sierras Exteriores): análisis estratigráfico integral y evolución sedimentaria. Zaragoza University (PhD Thesis; 345 pp.).
Taberner, C., Bosence, D.W.J., 1985. An Eocene biodetrital mud-mound from the southern Pyrenean foreland basin, Spain: an ancient analogue for Florida Bay mounds? In: Monty, C.L.V., Bosence, D.W.J., Bridges, P.H., Pratt, B.R. (Eds.), Carbonate Mud-Mounds - Their Origin and Evolution. IAS dpec. publ., pp. 423–437
Taberner, C., Dinarès-Turell, J., Giménez, J., Docherty, C., 1999. Basin infill architecture and evolution from magnetostratigraphy cross-basin correlations in the southeastern Pyrenean foreland basin. Geological Society of America Bulletin 11, 1155–1174.
Tabuce, R., Adnet, S., Cappetta, H., Noubhani, A., Quillevere, F., 2005. Aznag (Ouarzazate basin, Morocco), nouvelle localité à sélaciens et mammifères de l'Eocène moyen (Lutétien) d'Afrique. Bulletin de la Société Géologique de France 176, 381–400.
Tawfik, M., El-Sorogy, A., Moussa, M., 2016. Metre-scale cyclicity in Middle Eocene platform carbonates in northern Egypt: implications for facies development and sequence stratigraphy. Journal of African Earth Sciences 119, 238–255.
Tomás, S., Frijia, G., Bömelburg, E., Zamagni, J., Perrin, C., Mutti, M., 2016. Evidence for seagrass meadows and their response to paleoenvironmental changes in the early Eocene (Jafnayn Formation, Wadi Bani Khalid, N Oman). Sedimentary Geology 341, 189–202.
Tomassetti, L., Benedetti, A., Brandano, M., 2016. Middle Eocene seagrass facies from Apennine carbonate platforms (Italy). Sedimentary Geology 335, 136–149.
Tosquella, J., Serra-Kiel, J., 1998. Los nummulítidos (Nummulites y Assilina) del Paleoceno Superior-Eoceno Inferior de la Cuenca Pirenaica: Sistemática. Acta Geologica Hispanica 31, 37–159.
Ungaro, S., 1994. Nummulite morphological evolution. Studies on ecology and paleoecology of benthic communities. In: Matteucci, R., et al. (Eds.), Boll. Soc. Paleont. It.. spec. vol. 2, pp. 343–349
Vecsei, A., Sanders, D., Bernoulli, D., Eberli, G.P., Pignatti, J.S., 1998. Cretaceous to Miocene sequence stratigraphy and evolution of the Maiella carbonate platform margin, Italy. In: Hardenbol, J., Thierry, J., Farley, M.B., Jacquin, Th., de Graciansky, P.C., Vail, P.R. (Eds.), Mesozoic and Cenozoic Sequence Stratigraphy of European Basins: SEPM spec. publ. 60, pp. 53–74.
Vera, J.A., 2000. El Terciario de la Cordillera Bética: Estado actual de conocimientos. Revista Sociedad Geológica de España 13, 345–373.
Vlahovic, I., Tisljar, J., Velic, I., Maticec, D., 2005. Evolution of the Adriatic Carbonate Platform: palaeogeography, main events and depositional dynamics. Palaeogeography, Palaeoclimatology, Palaeoecology 220, 333–360.
Westerhold, T., Röhl, U., Donner, B., Frederichs, T., Kordesch, W.E.C., Bohaty, S.M., Hodell, D.A., Laskar, J., Zeebe, R.E., 2018. Late Lutetian Thermal Maximum-Crossing a thermal threshold in Earth's climate system? Geochemistry, Geophysics, Geosystems 19, 73–82.
Whidden, K., Jones, R.W., 2012. Correlation of early paleogene global diversity patterns of large benthic foraminifera with Paleocene and Eocene climatic events. Palaios 27 (3), 235–251.
Wildi, W., 1983. La chaîne tello-rifaine (Algérie-Maroc-Tunisie): structure, stratigraphie et évolution du Trias au Miocène. Revue Géologie: Dynamique Géographie Physique 24, 201–297.
Wilson, M., Vecsei, A., 2005. The apparent paradox of abundant formal facies in low latitudes: their environmental significance and effect on platform development. Earth-Science Reviews 69 (1), 133–168.
Zachos, J.C., Quinn, T.M., Salamy, K.A., 1996. High-resolution (104 yr) deep-sea foraminiferal stable isotope records of the Eocene-Oligocene climate transition. Paleoceanography 11, 251–266.
Zachos, J.C., Dickens, G.R., Zeebe, R.E., 2008. An early Cenozoic perspective on greenhouse warming and carbon-cycle dynamics. Nature 451, 279–283.